bioRxiv preprint doi: https://doi.org/10.1101/2023.07.26.550616; this version posted July 28, 2023. The copyright holder for this preprint (which was not certified by peer review) is the author/funder, who has granted bioRxiv a license to display the preprint in perpetuity. It is made available under aCC-BY 4.0 International license.

Sox3-null hypopituitarism depends on median eminence NG2-glia and is influenced by aspirin and gut microbiota

Christophe Galichet, Karine Rizzoti and Robin Lovell-Badge

Stem Cell Biology and Developmental Genetics Lab, The Francis Crick Institute, 1 Midland Road, London NW1 1AT

Authors for correspondence: robin.lovell-badge@crick.ac.uk, karine.rizzoti@crick.ac.uk and christophe.galichet@crick.ac.uk

The authors have declared that no conflict of interest exists.

Key words: median eminence, pituitary, NG2-glia, oligodendrocyte precursor cells, aspirin, gut microbiota

bioRxiv preprint doi: https://doi.org/10.1101/2023.07.26.550616; this version posted July 28, 2023. The copyright holder for this preprint (which was not certified by peer review) is the author/funder, who has granted bioRxiv a license to display the preprint in perpetuity. It is made available under aCC-BY 4.0 International license.

Abstract

The median eminence (ME), located at the base of the hypothalamus, is an essential centre of information exchange between the brain and the pituitary. We and others previously showed that mutations and duplications affecting the transcription factor *SOX3*/*Sox3* result in hypopituitarism, and this is likely of hypothalamic origin. We demonstrate here that the absence of *Sox3* predominantly affects the ME with phenotypes that first occur in juvenile animals, despite the embryonic onset of SOX3 expression. In the pituitary, reduction in hormone levels correlates with a lack of endocrine cell maturation. In parallel, ME NG2-glia renewal and oligodendrocytic differentiation potential are affected. We further show that low-dose aspirin treatment, which is known to affect NG2-glia, or changes in gut microbiota, rescue both proliferative defects and hypopituitarism in *Sox3* mutants. Our study highlights a central role of NG2-glia for ME function during a transitional period of post-natal development, and indicates their sensitivity to environmental signals.

bioRxiv preprint doi: https://doi.org/10.1101/2023.07.26.550616; this version posted July 28, 2023. The copyright holder for this preprint (which was not certified by peer review) is the author/funder, who has granted bioRxiv a license to display the preprint in perpetuity. It is made available under aCC-BY 4.0 International license.

Introduction

The hypothalamus is a crucial regulator of homeostasis and energy balance in vertebrates. It centralizes information from other regions of the brain and from the periphery, while an important part of its function is to regulate the secretion of pituitary hormones. These control essential functions, including post-natal growth, puberty, pregnancy, fertility, lactation, stress and energy homeostasis. Consequently, pituitary hormones deficiencies (hypopituitarism) are associated with significant morbidity.

The murine pituitary gland, which is located under the hypothalamus, has three compartments: the anterior pituitary lobe (AL), containing five different endocrine cell types, the intermediate (IL) with one (melanotrophs), and the posterior pituitary, composed of glial cells and hypothalamic axonal termini. The hypothalamus connects to the pituitary via the pituitary stalk, which itself contains neuronal, glial , and vascular components.

AL endocrine cells are regulated by neurohormones secreted by different hypothalamic neurons into a bed of fenestrated capillaries located at the base of the third ventricle, in a structure called the median eminence (ME). These neurohormones are delivered to the anterior pituitary by the hypophyseal portal system. Conversely, for the posterior pituitary, neurohormones (oxytocin and vasopressin) are released directly from hypothalamic axons that reach the gland itself (1). The ME, which is located outside the blood-brain barrier (2), and the pituitary stalk are crucial components of the hypothalamo-pituitary axis, as flow of information in and out of the hypothalamus is respectively collected and conveyed through these structures. In addition to the blood vessels, several cell types, including glial cells and microglia, are found in the ME (for review see (2, 3)). NG2-glia, or oligodendrocyte

bioRxiv preprint doi: https://doi.org/10.1101/2023.07.26.550616; this version posted July 28, 2023. The copyright holder for this preprint (which was not certified by peer review) is the author/funder, who has granted bioRxiv a license to display the preprint in perpetuity. It is made available under aCC-BY 4.0 International license.

precursor cells (OPCs), are present in ME (4-6). They are the most proliferative cells within the central nervous system (CNS) and their primary function is to generate oligodendrocytes, although rarely astrocytes and neurons in some contexts. However, they also fulfil other roles, such as interacting with and modulating the function of neighbouring neurons, astrocytes or microglia (for review see (7)). Within the ME, NG2-glia have been shown to generate oligodendrocytes (5, 6), some of which are in close contact with the dendrites of leptin receptor expressing neurons. The relevance of these interactions is revealed by ablation of ME NG2-glia which results in the degeneration of these dendrites, leading to increased body weight (4). Furthermore, refeeding after an overnight fast induces a rapid proliferation and differentiation of ME NG2-glia (6), demonstrating that nutrition influences, and is influenced by, ME NG2-glia. Another category of glial cells, the tanycytes, of which there are several types (8), are flanking the base of the third ventricle. Because the ME is located outside the blood-brain barrier, tanycytes are exposed to both the systemic circulation and the cerebro-spinal fluid (9). They regulate neurohormone secretion from hypothalamic axon terminals (10-12) and modulate the release of blood-borne peripheral information to the hypothalamus ((13) and for review see (14)). Furthermore, they comprise a population of hypothalamic stem cells (SCs) (for review see (2, 15)). Similarly to other CNS stem cell populations, tanycytes express the HMG-box transcription factor SOX2 (16-20), required for maintenance of several different adult stem cell populations (for review see (21)). In embryonic neural progenitors, SOX2 is often co-expressed with the two other SOXB1 members, SOX1 and SOX3 (22). Upon cell differentiation, either in embryonic or adult contexts, expression of *Soxb1* genes, tends to be downregulated (23). There are exceptions, however. For example, SOX2 and SOX3 are

bioRxiv preprint doi: https://doi.org/10.1101/2023.07.26.550616; this version posted July 28, 2023. The copyright holder for this preprint (which was not certified by peer review) is the author/funder, who has granted bioRxiv a license to display the preprint in perpetuity. It is made available under aCC-BY 4.0 International license.

maintained in spinal cord oligodendrocyte precursors, where they are required for their differentiation (24).

In both humans and mice, mutations in *SOX3/Sox3* are associated with hypopituitarism (for review see (25)). In mice, we showed that SOX3 is largely absent from the pituitary, but it is found in the developing and mature hypothalamus, being particularly highly expressed in the embryonic infundibulum and later maintained in the ME ((26) and this study). Here, we aimed to characterise the role of SOX3 in the hypothalamus and the etiology of the hypopituitarism. Using conditional gene deletion, we show that loss of *Sox3* in the central nervous system (CNS) is sufficient to cause hypopituitarism and that this develops postnatally, at the time of weaning. Consequently, we observe in the pituitary a defective maturation of endocrine cells. SOX3 is expressed in hypothalamic stem cells and its deletion affects their proliferation *in vivo* and in hypothalamic neurosphere assays. SOX3 is also expressed in NG2-glia in the ME, and both their proliferation and differentiation are reduced in *Sox3* mutants. Furthermore, we observe a striking deficiency in myelination of axons in the ME. Importantly, the appearance of all these defects correlates with development of hypopituitarism suggesting that SOX3 is required postnatally for the functional maturation of the ME. Building on previous work demonstrating the efficacy of aspirin in inducing proliferation and/or differentiation of NG2-glia (27, 28), we treated *Sox3* mutants with low dose aspirin. We observed a restoration of NG2-glia proliferation, and a rescue of pituitary hormonal deficiencies, but not a rescue of myelination. We also found that changes in the gut microbiome ameliorate the hypopituitarism. Our study highlights a novel role for NG2-glia in the post-weaning formation of a functional ME and

bioRxiv preprint doi: https://doi.org/10.1101/2023.07.26.550616; this version posted July 28, 2023. The copyright holder for this preprint (which was not certified by peer review) is the author/funder, who has granted bioRxiv a license to display the preprint in perpetuity. It is made available under aCC-BY 4.0 International license.

its control of pituitary maturation, and that an otherwise robust phenotype due to loss of *Sox3* in these cells can be modified by non-genetic factors.

Results

1. SOX3 is required in the hypothalamus for post-natal pituitary endocrine cell maturation.

SOX3 is widely expressed in the developing CNS (22), but it is also retained within some brain regions postnatally, notably the hypothalamus (26), where its expression is found in neural stem cells (NSCs) and several differentiated cell types (29) (Fig 2.A-F). In contrast, we only observed SOX3 in rare cells within the pituitary representing a very small subset of lactotrophs (Supplementary Fig.1A). Therefore, the hypopituitarism displayed by *Sox3* mutants is likely to be of hypothalamic origin.

To test this hypothesis, we used *Nestin-Cre* (30) and *Pou1f1-Cre* (31) to delete *Sox3* in the CNS and the pituitary respectively. Pituitary hormonal contents were then measured by radio immunoassay (RIA) in two-month-old males (Fig.1A). While *Nestin*-Cre animals display a modest but significant reduction in GH levels, as we previously reported (32), we observed a significant reduction of growth hormone (GH) contents in *Nestin*-Cre*; Sox3*$^{floxGFP/Y}$ mice compared to both *Nestin*-Cre and *Sox3*$^{floxGFP/Y}$ controls. This 75% reduction in *Nestin*-Cre*; Sox3*$^{floxGFP/Y}$ mice is comparable to the one measured in *Sox3*$^{-/Y}$ mutant males (Fig.1A, (26)). In contrast, in *Pou1f1*-Cre*; Sox3*$^{floxGFP/Y}$ mice, neither GH (Fig.1A) nor Prolactin (PRL) (Supplementary Fig.1B) contents are affected. These data are therefore in agreement with a CNS origin of the hypopituitarism displayed by *Sox3*-null

bioRxiv preprint doi: https://doi.org/10.1101/2023.07.26.550616; this version posted July 28, 2023. The copyright holder for this preprint (which was not certified by peer review) is the author/funder, who has granted bioRxiv a license to display the preprint in perpetuity. It is made available under aCC-BY 4.0 International license.

animals. To avoid undesirable effects originating from the *Nestin*-Cre transgene, we pursued our subsequent analyses on *Sox3*-null animals.

We then measured GH contents at different time points after birth to determine when deficits appear in *Sox3*-null males (Fig.1B). After birth, GH levels rise normally in mutants compared to controls, but decline sharply shortly after weaning, down to 25% of the levels observed in controls at two months of age. Similar post-weaning deficiencies were measured for PRL, TSH and LH (Supplementary Fig.1C; (26)). Because the growth spurt observed in juveniles is known to be regulated by changes in GHRH pulsatility (33), this result is again in accord with a hypothalamic origin of the phenotype in *Sox3*-null animals.

We did not observe any obvious morphological defect in the hypothalami in *Sox3*-null adult males (26). We thus examined in more detail the arcuate and paraventricular nuclei, both involved in GH secretion control, by performing *in situ* hybridisation using *growth hormone releasing hormone* (*Ghrh*) and *somatostatin* (*Sst*) mRNA probes (Fig.1C). Their expression patterns are similar in control and mutants, again indicating that cell specification and patterning within the hypothalamus are unaffected.

To understand which aspect of hypothalamic function is affected in mutants, we examined the consequences of *Sox3* loss in the pituitary. In parallel with the appearance of the hormonal deficiencies, we observed that the growth of the anterior lobe slows down significantly in mutants compared to controls after weaning (Fig.1D). Furthermore, while the cellular density in control animals sharply decreases between 4 and 5 weeks of age, it remains constant in mutants (Fig.1E). This suggests that endocrine cells, whose secretory capacities usually increase dramatically postnatally (34), remain small in *Sox3* mutants. To confirm this hypothesis, we measured the volume of TSH secreting cells. We chose these

bioRxiv preprint doi: https://doi.org/10.1101/2023.07.26.550616; this version posted July 28, 2023. The copyright holder for this preprint (which was not certified by peer review) is the author/funder, who has granted bioRxiv a license to display the preprint in perpetuity. It is made available under aCC-BY 4.0 International license.

because they represent a small population, about 5% of AL cells (35), and because they are individualized, which thus make them suitable for cell volume measurement. In control animals, TSH positive cells double their volume from one-week old to adulthood. In contrast, in *Sox3* mutants, their volume does not significantly increase during the same period (Fig.1F). This suggests that hormonal secretory capacity/maturation is affected in mutants. We directly examined this aspect by performing transmission electron microscopy (TEM) and observed a striking reduction in the number of secretory granules in cells of *Sox3*-null ALs (Fig.1G), implying impaired endocrine cell terminal differentiation. Altogether these data show that the hypopituitarism displayed by *Sox3*-null mice is of hypothalamic origin. The consequence, at the pituitary level, is an impairment of endocrine cell maturation, which becomes apparent after weaning and results in the production of insufficient levels of hormones.

2. Hypothalamic progenitor maintenance *in vitro* relies on SOX3.

To determine the origin of the hypothalamic defect, we analysed SOX3 expression in more detail (Fig.2A). SOX3 is expressed in cells lining the third ventricle and in scattered cells in the surrounding parenchyma. In the latter, it is present in some neurons (NeuN, Fig.2B), as previously shown (29), and in a few astrocytes (GFAP, Fig.2C) and NG2-glia (PDGFRa, Fig.2E-F). SOX3 is also present in Nestin^{+ve} tanycytes (Fig.2D). Within the ME, SOX3 is found in NG2-glia (PDGFRa, Fig.2E; NG2, Supplementary Fig.2A), but not in MAG^{+ve} oligodendrocytes (Supplementary Fig.2B).

Because SOX3 is expressed in hypothalamic NSCs, and SOXB1 proteins are known to be required for NSC emergence and maintenance (for review see (21)), we first performed *in*

bioRxiv preprint doi: https://doi.org/10.1101/2023.07.26.550616; this version posted July 28, 2023. The copyright holder for this preprint (which was not certified by peer review) is the author/funder, who has granted bioRxiv a license to display the preprint in perpetuity. It is made available under aCC-BY 4.0 International license.

situ hybridization for the tanycyte marker *Rax* (36). We did not observe any difference in *Rax* expression pattern between *Sox3* mutants and control animals, suggesting that deletion of *Sox3* does not affect tanycyte emergence (Fig.2G). We then investigated neurosphere forming ability of hypothalamic progenitors from 6-week-old animals (37) (Fig.2H). We generated *Sox3*$^{+/Y}$ hypothalamic neurospheres which maintain expression of SOX3 (Fig.2Hiii), as previously shown for embryonic ones (38). Neurospheres from *Sox3*-null hypothalamic progenitors were formed and these express GFP, the open reading frame of which replaces that of *Sox3* (Fig.2Hiv) (26). There was initially no difference in the number of plated cells and of primary neurospheres formed between control and mutants. However, by the third passage, the total number of cells and size of *Sox3* mutant spheres had declined sharply (Fig.2H-I – red lines). In subsequent passages, most *Sox3*-null cells adhere and very few neurospheres are formed, with none arising by the 9th passage. We then analysed cell proliferation and apoptosis on adherent NSC cultures of dissociated neurospheres (39). There were significantly fewer phospho-histone H3^{+ve} mitotic cells in *Sox3*-null samples (Fig.2J) while no increase in cell apoptosis was observed by TUNEL assay (Supplementary Fig.3A). In contrast, formation and maintenance of neurospheres from the sub-ependymal zone (SEZ), a well characterised adult neurogenic niche (40), which also express SOX3 (41), is normal in adult *Sox3* mutants (Fig.2I – blue lines). Furthermore, hypothalamic neurospheres made from *Sox3*-null mutants before the hypopituitarism appears can also be propagated and proliferate normally (Supplementary Fig.4A, B). We analysed the differentiation potential of pre and post-weaning hypothalamic NSCs *in vitro* (Supplementary Fig.5A-B). As previous shown (19, 38), we observed differentiation into the three CNS lineages, βIII-tubulin^{+ve} neurons, GFAP^{+ve} astrocytes and CNPase^{+ve}

bioRxiv preprint doi: https://doi.org/10.1101/2023.07.26.550616; this version posted July 28, 2023. The copyright holder for this preprint (which was not certified by peer review) is the author/funder, who has granted bioRxiv a license to display the preprint in perpetuity. It is made available under aCC-BY 4.0 International license.

oligodendrocytes in control and *Sox3* mutants. Therefore, SOX3 is necessary for self-renewal, but not differentiation *in vitro*, in hypothalamic neurospheres and this requirement correlates in time with the onset of hypopituitarism in mutant animals.

We next performed neurosphere assays using *Sox3*$^{+/\Delta GFP}$ females (Fig.2K). Due to the location of *Sox3* on the X-chromosome and to random X chromosome inactivation, cells from these mice that normally transcribe *Sox3* should express either SOX3 or GFP in roughly equal proportions. This was seen in neurospheres derived from the SEZ of two-month- or ten-day old *Sox3*$^{+/\Delta GFP}$ animals and in spheres derived from the hypothalamus of ten-day old *Sox3*$^{+/\Delta GFP}$ pups cultured in non-clonal conditions (Fig.2K and Supplementary Fig.4C). In contrast, neurospheres from the hypothalamus of two-month-old *Sox3*$^{+/\Delta GFP}$ animals, show a significant reduction in the contribution of GFP^{+ve}, *Sox3*-null cells, compared to SOX3^{+ve}, GFP^{-ve} cells (Fig.2K). This mosaic analysis confirms and expands our previous analyses, showing that SOX3 is required cell-autonomously for hypothalamic NSC self-renewal *in vitro*, again, in a age-dependent manner.

3. SOX3 is required in the ME for cell renewal.

We then examined cell proliferation *in vivo* by performing BrdU incorporation experiments. In *Sox3*$^{+/Y}$ adult hypothalami, we observed BrdU^{+ve} cells within the ME and the parenchyma (Fig.3B), as previously shown (for review see (14, 42)). In both control and mutant adult hypothalami, BrdU^{+ve} cells are mostly located within the body of the ME rather than in ventricle lining cells (Fig.3B). We observed fewer BrdU^{+ve} cells in mutants versus controls (Fig.3B-C), predominantly affecting the ME where a 40% reduction in BrdU incorporation/ME surface area is observed in mutants (Fig.3D). ME is also

bioRxiv preprint doi: https://doi.org/10.1101/2023.07.26.550616; this version posted July 28, 2023. The copyright holder for this preprint (which was not certified by peer review) is the author/funder, who has granted bioRxiv a license to display the preprint in perpetuity. It is made available under aCC-BY 4.0 International license.

significantly smaller in mutants (Fig.3D). Because we did not observe any increase in the number of apoptotic cells in *Sox3* mutants compared to controls (Supplementary Fig.3B), the smaller size of the ME is likely explained by its reduced proliferative capacity. In contrast, BrdU incorporation in the dentate gyrus, another well studied neurogenic niche (40), of 2-month-old mutants is similar to that of controls (Fig.3C). There was also no difference in the number of $BrdU^{+ve}$ cells in 1-week-old hypothalami between control and *Sox3* mutant littermates, i.e. before the hypopituitarism appears in the latter (Supplementary Fig.4D).

Immunochemistry was used to analyse the identity of the proliferating cells in the ME. In controls, the vast majority of $BrdU^{+ve}$ cells express SOX3, SOX2 and one or more of the SOXE proteins SOX8, SOX9 and SOX10 (80, 75 and 82% of $BrdU^{+ve}$ cells respectively, Fig.3F-G). These cells also express NG2-glia markers such as PDGFRa and OLIG2 (65 and 80% of $BrdU^{+ve}$ cells respectively Fig.3F-G), in agreement with studies showing that NG2-glia are the most proliferative cell type in the ME (4, 43). In *Sox3* mutants, the remaining $BrdU^{+ve}$ cells also represent NG2-glia (Fig.3G), although their proliferation is significantly affected in the ME (Fig.3E).

In summary, SOX3 is required for cell renewal within the ME. Within this structure, NG2-glia proliferation is particularly sensitive to *Sox3* deletion. Moreover, in agreement with an impairment of neurosphere maintenance (Fig.2), proliferation of tanycytes is also affected in mutants (Fig.3C). The reduction in ME cell renewal correlates with the onset of hypopituitarism in mutants.

4. SOX3 supports ME oligodendrocyte differentiation.

bioRxiv preprint doi: https://doi.org/10.1101/2023.07.26.550616; this version posted July 28, 2023. The copyright holder for this preprint (which was not certified by peer review) is the author/funder, who has granted bioRxiv a license to display the preprint in perpetuity. It is made available under aCC-BY 4.0 International license.

Because NG2-glia represent the ME cell population mostly affected by *Sox3* deletion, we next characterised their differentiation potential in mutants by performing lineage tracing in *Pdgfra*-CreERT2; *Rosa26*^{ReYFP} animals. In six-week-old control mice, the majority of eYFP^{+ve} cells detected four weeks after tamoxifen induction are PDGFRa and OLIG2 positive NG2-glia, both in the hypothalamic parenchyma and ME (Fig.4B-C). In the latter, 20% of the eYFP^{+ve} cells have become MAG^{+ve} mature oligodendrocytes. In contrast, in *Sox3*-null mutants, we observed a significant reduction in the percentage of MAG^{+ve} oligodendrocytes in the progeny of PDGFRa^{+ve} precursors compared to controls, while there is an increase in the proportion of eYFP; PDGFRa-double positive cells in ME (Fig.4B-C). These results suggests that ME PDGFRa^{+ve} progenitors are unable to differentiate into oligodendrocytes in the absence of SOX3. We thus examined these cells in the ME. We found both fewer PDGFRa^{+ve} progenitors and mature MAG^{+ve} oligodendrocytes in 2-month-old *Sox3*-null ME compared to controls (Fig.4D). The reduction in PDGFRa^{+ve} cell numbers is in agreement with a reduction in proliferation (Fig.3C), while the decrease in MAG^{+ve} oligodendrocytes fits with an impaired differentiation capacity. We also noticed an increase in cells expressing APC, which is not expressed by NG2-glia, but is a marker of both differentiating and differentiated oligodendrocytes (5). This indicates that immature oligodendrocytes accumulate in the mutant ME, reflecting a role for SOX3 post weaning in both early and late stages of this lineage (Fig.4D). To confirm the latter, we analysed myelination by transmission electron microscopy (TEM) (Fig.4E). Myelinated axons are clearly visible in control hypothalamic parenchyma and ME, and in the parenchyma of *Sox3* mutants, however we could not observe any in the mutant ME, in agreement with defective oligodendrocytic

bioRxiv preprint doi: https://doi.org/10.1101/2023.07.26.550616; this version posted July 28, 2023. The copyright holder for this preprint (which was not certified by peer review) is the author/funder, who has granted bioRxiv a license to display the preprint in perpetuity. It is made available under aCC-BY 4.0 International license.

differentiation. Collectively, this data allows us to hypothesise that the reduced number of NG2-glia and/or the lack of myelination explain the reduction in pituitary hormone levels in SOX3 mutants.

5. Aspirin treatment rescues hypothalamic and pituitary defects in *Sox3* mutants.

Two reports have suggested that aspirin can specifically affect NG2-glia (27, 28) In one, both proliferation and differentiation of NG2-glia were induced by low dose aspirin administration *in vitro* and *in vivo* following an ischemic injury in rats (28), while the second suggests that differentiation was exclusively enhanced in neonates following treatment (27). We therefore decided to examine the effects of a low dose aspirin treatment (12mg/day/kg for 21 days) in 2-month old *Sox3*-null animals. We first examined BrdU incorporation within ME and observed a significant rescue of the proliferation defect, with the number of $BrdU^{+ve}$ cells/section being now similar between control and aspirin treated mutants (Fig.5A-C). We then examined the composition of the ME with respect to the oligodendrocyte lineage. We observed a significant increase of $PDGFRa^{+ve}$ cells, and a decrease of APC^{+ve} cells in aspirin treated compared to untreated *Sox3*-null mice (Fig.5B-D). However, we did not observe any significant increase in MAG^{+ve} cells or myelination of axons in the ME with aspirin treatment (Fig.5D, Supplementary Fig.6A). Finally, we examined pituitary GH (Fig.5E) and ACTH (Supplementary Fig.6B) levels and observed a clear and significant rescue of the deficiencies in aspirin treated *Sox3*-null mice. These data show that aspirin is able to restore proliferation of NG2-glia and pituitary function, but that the latter does not depend on differentiation to mature oligodendrocytes or myelination of axons.

bioRxiv preprint doi: https://doi.org/10.1101/2023.07.26.550616; this version posted July 28, 2023. The copyright holder for this preprint (which was not certified by peer review) is the author/funder, who has granted bioRxiv a license to display the preprint in perpetuity. It is made available under aCC-BY 4.0 International license.

6. Pituitary function in *Sox3* mutants is sensitive to composition of gut microbiota

Following our relocation to the Francis Crick institute (Crick) from the National Institute for Medical Research (NIMR), the hypopituitarism was no longer seen in rederived *Sox3*-null mice (Fig. 6D), while the cranio-facial defects (44) were still present. There were several differences between the new mouse facility and the previous one, ranging from water to cage system, but notably these included the adoption of a free-from animal protein and fish meal diet (supplementary Fig.7). Because an increasing number of studies have highlighted the relationship between diet and gut microbiome and, in turn, gut microbiome and hypothalamic functions (for review see (45-47)), we compared the gut microbiota of mice hosted in our previous and current institutions. At the phylum level, we found substantial differences, with Bacteroidetes more abundant at NIMR, while Firmicutes were prominent at the Crick (Fig.6A) leading to a F/B ratio of 0.25±0.2 at NIMR and of 2.22±0.532 at the Crick (Fig.6B). At the species level, the alpha diversity was reduced at the Crick compared to NIMR (Fig.6C). To test whether changes in gut microbiota underlie rescue of hormonal deficiencies, we performed faecal transplant (FT) from NIMR animals into Crick animals. Transplants were successful, with FT mice displaying phylum abundance, F/B ratio and alpha diversity similar to that of NIMR mice (Fig.6A-C). Notably this was accompanied by reappearance of the hypopituitarism, with *Gh* expression being reduced in *Sox3*-null FT animals compared to controls (Fig.6D). We then analysed the oligodendrocyte lineage, particularly in the ME, of NIMR, Crick and FT control and *Sox3*-null animals. The reduction in the number of PDGFRa^{+ve} NG2-glia and concomitant increase of APC^{+ve} cells observed in NIMR *Sox3*-null mice (Fig.5B-D and Fig.6E-F) was

bioRxiv preprint doi: https://doi.org/10.1101/2023.07.26.550616; this version posted July 28, 2023. The copyright holder for this preprint (which was not certified by peer review) is the author/funder, who has granted bioRxiv a license to display the preprint in perpetuity. It is made available under aCC-BY 4.0 International license.

confirmed in FT *Sox3*-null ME but absent in Crick *Sox3*-null ME (Fig.6E-F). Altogether, these data indicate that changes of gut microbiota affect oligodendrocyte lineage composition in ME, and occurrence of hypopituitarism in *Sox3*-null mutants.

In conclusion, because NG2-glia in the ME are the cells mostly affected by *Sox3* loss and their proliferation, but not differentiation to oligodendrocytes, is corrected by either low-dose Aspirin treatment or by a 'Crick-typical' profile of gut microbiota, we propose that sufficient numbers of NG2-glia are required in the ME to support pituitary cell maturation as the animal becomes independent at weaning.

Discussion

Congenital pituitary hormone deficiencies, found with a frequency of about 1/4000 (48), can significantly affect quality of life. However, relatively few genes have been identified as being causative, with most of these having critical roles in prenatal pituitary development (48-50). Moreover, ways to treat patients are limited to replacement of missing hormones, but in way that does not mimic their normal physiological release by the pituitary. Mutations affecting SOX3 are associated with panhypopituitarism in mice and humans (25, 26), however the etiology of this remains unknown. We show here that the phenotype displayed by *Sox3*-null mice is of hypothalamic origin. Specifically, we find defects in the median eminence (ME) lead to a failure of endocrine cell maturation in the pituitary, which normally occurs after weaning, resulting in the production of insufficient levels of hormones.

The ME of the hypothalamus is a crucial structure conveying information from and to the brain, but how and when it becomes functional and controls pituitary output is not well

bioRxiv preprint doi: https://doi.org/10.1101/2023.07.26.550616; this version posted July 28, 2023. The copyright holder for this preprint (which was not certified by peer review) is the author/funder, who has granted bioRxiv a license to display the preprint in perpetuity. It is made available under aCC-BY 4.0 International license.

characterized (51-55). We find that SOX3 is required for self-renewal of both hypothalamic NSCs, which are part of the tanycyte population lining the third ventricle including the ME, and NG2-glia within the ME. SOX3 is also required for the differentiation of the latter to mature oligodendrocytes, however in two conditions where the panhypopituitarism is rescued, via the effects of aspirin or altered gut microbiota, although cell proliferation returns to normal, there is still a failure of oligodendrocyte differentiation suggesting that myelination of axons is not essential for ME function. Given that the hypothalamic NSCs generate very few neurons, if any, post-puberty (for review see (56)), it would seem most likely that the pituitary phenotype is due to insufficient numbers of glia. Indeed, our data implicates the NG2-glia themselves as having a critical role in inducing or allowing pituitary endocrine cell maturation. It follows that there must be processes that occur around weaning in the ME, perhaps involving an increase in levels and/or alteration in patterns of hormone releasing factors secreted into the hypophyseal portal system, which are indispensable for function of the juvenile pituitary.

Weaning is a crucial transition period when the suckling pup becomes independent (57) and this is accompanied by both behavioural and physiological changes (58). The sensitivity of this stage is highlighted by mutations in genes affecting appetite control, another crucial function of the hypothalamus (59), such as in *Neurogenin3* (60) and U11 spliceosomal RNA (*Rnu11*) (61), or affecting the maturation of endocrine cells in the pancreas (62). It would of interest to ask if altering the time of weaning of *Sox3*-null mice has any influence on the onset of pituitary hormone deficiencies.

SOX3 in hypothalamic neural stem cells

bioRxiv preprint doi: https://doi.org/10.1101/2023.07.26.550616; this version posted July 28, 2023. The copyright holder for this preprint (which was not certified by peer review) is the author/funder, who has granted bioRxiv a license to display the preprint in perpetuity. It is made available under aCC-BY 4.0 International license.

We show that tanycytes, a proportion of which are hypothalamic neural stem cells, divide less frequently in *Sox3*-null mice compared to controls. This is also reflected in neurosphere cultures derived from the hypothalamus, where those from *Sox3*-null mice post-weaning fail to be maintained for more than a few passages in contrast to cultures initiated at earlier stages or from other neurogenic niches at any stage. This is similar to the effects of the loss of *Sox2* in the adult dentate gyrus (63). We showed that lineage commitment is not affected in differentiated *Sox3*-null hypothalamic neurospheres, consistent with a previous report indicating that over-expression of SOX3 does not promote neurogenesis in embryonic telencephalic NSC culture (64). This is in contrast with SOX1 and SOX2, the other members of the SOXB1 family, which have essential roles in neuronal differentiation (63, 65).

SOX3 is present in all adult NSC niches ((41) and this study), however, its loss exclusively affects hypothalamic stem/progenitor cells post puberty. In the embryonic brain, SOX3 is expressed at its highest levels in the infundibulum which will give rise to the ME. Although the related factor SOX2, with which it is known to show functional redundancy, is expressed throughout the neuroepithelium, the absence of SOX3 does have consequences at this stage with respect to induction of the pituitary and its morphological development (26). It seems likely that the hypothalamic stem cells, in which SOX2 is also expressed, are similarly more sensitive to the loss of SOX3.

Sox3 and ME NG2-glia

NG2-glia are the most clearly affected cell type in the *Sox3*-null ME, with both their proliferation and differentiation being disrupted, which suggests that deficits in this

bioRxiv preprint doi: https://doi.org/10.1101/2023.07.26.550616; this version posted July 28, 2023. The copyright holder for this preprint (which was not certified by peer review) is the author/funder, who has granted bioRxiv a license to display the preprint in perpetuity. It is made available under aCC-BY 4.0 International license.

population are responsible for the hypopituitarism. We cannot exclude an additional role for tanycytes, whose maintenance is also affected in *Sox3* mutants, however, hypothalamic stem cells do not normally give rise to NG2-glia in adult mice (66); it is therefore unlikely that the reduction in the number of ME NG2-glia in *Sox3* mutants is secondary to the proliferation defect of the stem cells. SOX3 function in ME NG2-glia could relate to its role in the spinal cord where it is required for their differentiation (24). ME NG2-glia proliferate faster than their parenchymal counterparts (5), perhaps because they are exposed to systemic blood circulation. This higher cell-turnover suggests that modest defects affecting this population may be more pronounced in the ME explaining why the defects seen in *Sox3* nulls are restricted to this domain.

Alternatively, rather than just being precursors of oligodendrocytes, NG2-glia have other roles that involve crosstalk with neurons, astrocytes and microglia (for review, see (7)), all of which are found within the ME (6). Indeed, a direct role for NG2-glia in the ME for neuronal function has already been indicated, whereby their ablation is associated with obesity attributed to degeneration of the dendritic processes of arcuate nucleus leptin receptor neurons (4). While we do not yet know if NG2-glia are required for pituitary hypophysiotropic neuron integrity, it is worth noting that hypopituitarism occurs in both humans and rats after cranial irradiation (67, 68) where NG2-glia may be the most sensitive cell type given their high rate of proliferation compared to other cell types in the brain.

Aspirin restores pituitary function in Sox3 mutants

A further indication that the hypopituitarism seen in the *Sox3* mutants is due to a deficiency of NG2-glia comes from the restoration of both pituitary function and proliferation of NG2-

bioRxiv preprint doi: https://doi.org/10.1101/2023.07.26.550616; this version posted July 28, 2023. The copyright holder for this preprint (which was not certified by peer review) is the author/funder, who has granted bioRxiv a license to display the preprint in perpetuity. It is made available under aCC-BY 4.0 International license.

glia with low dose aspirin, while differentiation into mature oligodendrocytes is still impaired. The canonical mode of action of low dose aspirin involves the suppression of cyclooxygenase (COX) 1 activities (69). COX1 is expressed in microglia (70) and tanycytes (71) and its inhibition in these could affect NG2-glia. However, it was shown recently that targeted ablation of microglia led to a decrease in NG2-glia, differentiating and mature oligodendrocytes in the ME (5) and indicated a relationship between microglia and myelin turnover. Detailed analyses would be needed to determine whether inhibition of COX1 activities in microglia by aspirin is responsible for the restoration of NG2-glia proliferation in *Sox3* mutants or if COX-independent mechanisms are also relevant (72). In contrast, low dose aspirin increases differentiation rather than proliferation of cultured NG2-glia by inhibiting Wnt signalling (27), but the situation may be different *in vivo*, where the effects of aspirin might also be mediated by other cells within or outside the ME.

Gut microbiota and hypopituitarism in Sox3 mutant mice

We found that changes in microbiome composition can alter both the NG2-glia phenotype and development of hypopituitarism in *Sox3* mutants. Communication between the gut microbiota and the brain could be via chemical compounds released into the blood stream, neuronal signalling, or by cells of the immune system (73). For example, changes on the gut microbiome affect circulating levels of the promyelinating factor IGF1, which in turn affects cortical myelin basic protein but not NG2 expression (74, 75). Moreover, it is now thought that an intact gut microbiota is necessary for a proper response from the hypothalamo-pituitary-adrenal axis. Indeed, germ-free mice, which have a minimal gut microbiota, display an exacerbated response to early life stress (76). It may be noteworthy

bioRxiv preprint doi: https://doi.org/10.1101/2023.07.26.550616; this version posted July 28, 2023. The copyright holder for this preprint (which was not certified by peer review) is the author/funder, who has granted bioRxiv a license to display the preprint in perpetuity. It is made available under aCC-BY 4.0 International license.

that gut microbiome composition changes drastically during early postnatal life, and only stabilises after weaning, which is when the absence of SOX3 becomes relevant (77). Understanding how a post-weaning stabilised microbiota of a particular composition could rescue both NG2-glia in the ME and pituitary deficiencies will be important especially if this can be shown to be relevant in humans.

In this respect, a 'weaning reaction' to microbiota has been described, and while this was associated with development of the immune system and protection against immunopathologies (78), gut bacterial cell wall components, muropeptides, can also be sensed directly via Nod1 and Nod2 receptors on cells in the brain, including the hypothalamus (79). It is worth noting that the predominant phylum of gut microbiota at NIMR were Gram negative Bacteroidetes, which possess a unique diaminopimelate-containing GlcNAc-MurNAc tripeptide muropeptide (GM-TriDAP) sensed by NOD1, while the most abundant phyla at the Crick are Gram-positive Firmicutes carrying the GlcNAc-MurNAc dipeptide (GM-Di), which can be sensed by both NOD1 and NOD2 (80-82). It will be important to determine which cells in the ME are expressing NOD1 and NOD2, especially post-weaning, and how these may respond to the different muropeptides. This might provide an explanation for the sensitivity of the *Sox3* pituitary phenotype to gut microbiota.

Conclusions

bioRxiv preprint doi: https://doi.org/10.1101/2023.07.26.550616; this version posted July 28, 2023. The copyright holder for this preprint (which was not certified by peer review) is the author/funder, who has granted bioRxiv a license to display the preprint in perpetuity. It is made available under aCC-BY 4.0 International license.

The data presented here strongly suggest that NG2-glia in the ME, and the presence of SOX3 in these, are crucial to forming a functional hypothalamo-pituitary axis post-weaning. Moreover, while hypopituitarism seen in both mice and humans lacking SOX3 can be a robust phenotype, we find that it can be modified by external influences, namely by low dose aspirin or gut microbiota. Consequently, because of the potential link between reduced NG2-glia after irradiation and hypopituitarism, it is of interest to explore whether low dose aspirin treatment and/or changes in microbiota composition could have rescuing effects in this context too.

Materials and methods.

Mice

Mice carrying the *Sox3*-conditional allele (*Sox3*$^{floxGFP/Y}$ – MGI:5550577**)** and *Sox3*-null allele, where the *Sox3* open reading frame is replaced by that of *gfp*, (*Sox3*$^{\Delta GFP/Y}$ referred as *Sox3*$^{-/Y}$ – MGI: 3036671)(26), and alleles for *Pou1f1*-Cre (31), *Nestin*-Cre (MGI: 2176222)(30), *Pdgfra*-CreERT2 (MGI: 3832569) (83), *Rosa26*^{ReYFP} (MGI: 2449038) (84) are maintained on MF1 background (random bred, NIMR:MF1 or HsdOla:MF1 for Crick and FT *Sox3*-null) and genotyped as described or by Transnetyx. All experiments carried out on mice were approved under the UK Animal (scientific procedures) Act (Project licence 80/2405, 70/8560 and PP8826065).

Radioimmunoassay

bioRxiv preprint doi: https://doi.org/10.1101/2023.07.26.550616; this version posted July 28, 2023. The copyright holder for this preprint (which was not certified by peer review) is the author/funder, who has granted bioRxiv a license to display the preprint in perpetuity. It is made available under aCC-BY 4.0 International license.

Pituitaries were homogenized in phosphate-buffered saline and anterior pituitary hormonal contents measured by radioimmunoassay (RIA) (85) using National Hormone and Pituitary Program reagents kindly provided by A.L. Parlow.

Neurosphere forming assay and monolayer culture

Hypothalamus and sub-ependymal zone (SEZ) were dissected and cultivated in proliferation medium as described previously (37, 86). Neurospheres were passaged using TrypLE™ express (Invitrogen). For monolayer culture, coverslips were coated with reduced growth factor matrigel (BD biosciences) and cells were plated at 2.10^4cells/ml.

Substance administration, sample processing and histology

BrdU (Sigma) and Tamoxifen (Sigma) were administered intraperitoneally at 100µg/g and 0.2mg/g body weight respectively twice daily for BrdU, and daily for Tamoxifen for 5 consecutive days. Adult animals were perfused intracardially with chilled 4% paraformaldehyde, brains were embedded in 2.5% agarose and free-floating sections obtained using a vibratome (Leica). Neurospheres or cell monolayers were fixed with chilled 4% paraformaldehyde for 20 minutes on ice. For histology, samples were fixed in Bouin's solution, processed for wax embedding, sectioned, and stained with haematoxylin and eosin.

Immunofluorescence, in situ hybridisation, TUNEL assay and qPCR experiments

Immunofluorescence was performed on 50µm free-floating sections, neurospheres or cell monolayers plated on coverslips. Samples were incubated in blocking solution (PBS, 10%

bioRxiv preprint doi: https://doi.org/10.1101/2023.07.26.550616; this version posted July 28, 2023. The copyright holder for this preprint (which was not certified by peer review) is the author/funder, who has granted bioRxiv a license to display the preprint in perpetuity. It is made available under aCC-BY 4.0 International license.

donkey serum, 0.1% Triton X-100) and primary antibodies were incubated overnight at 4ºC (Table 1). Detection was performed using a 1:500 dilution of anti-rabbit, anti-mouse or anti-goat secondary antibodies conjugated to Alexa-488, Alexa-555, Alexa-594 or Alexa-647 (Molecular probes). DNA was labelled using DAPI and sections were mounted in Aquapolymount (polysciences). RNA *in situ* hybridization on free-floating sections was performed as previously described (87) using *Rax* (88), *Ghrh* and *somatostatin* probes (gift from JP. Martinez-Barbera, ICH, UCL, UK). TUNEL experiments were carried out following the supplier manual (ApopTag Kit, Millipore). For gene expression, RNA extraction was carried out following the supplier manual (miRNeasy kit, Qiagen). Complementary DNA was synthetised using 1x qScript cDNA SuperMix (Quantabio). Quantitative PCR (qPCR) were performed using PowerUp SYBR green (ThermoFisher Scientific) with primers for *Gh* 5'TGGGCAGATCCTCAAGCAAACCTA3' and 5'GAAGGCACAGCTGCTTTCCACAAA3'. Glyceraldehyde 3-phosphate dehydrogenase (GAPDH) expression was used as house-keeping gene (5'TTCACCACCATGGAGAAGGC3' and 5'CCCTTTTGGCTCCACCCT3'). Each biological sample was run in technical triplicates and, at least, three biological samples were analysed. Relative expression of gene of interest was calculated according to the ddCt method (89) and represented as fold change to the corresponding control.

Faecal transplant and gut microbiota sequencing

Crick mice were rederived into germ-free condition. Homogenised NIMR faecal materials in PBS were administered by oral gavage (TruBIOME, Taconic). Freshly collected or snap-

bioRxiv preprint doi: https://doi.org/10.1101/2023.07.26.550616; this version posted July 28, 2023. The copyright holder for this preprint (which was not certified by peer review) is the author/funder, who has granted bioRxiv a license to display the preprint in perpetuity. It is made available under aCC-BY 4.0 International license.

frozen faecal materials were incubated in stabilisation buffer and whole genome sequenced (Transnetyx); Data was analysed with OneCodex software.

Quantification and statistical analysis

Images were captured by confocal microscopy (Leica SP5 or SPE) or by light microscope (Leica DMRA2) and analysed using Leica LAS AF, ImageJ, OpenLab or Volocity softwares. For anterior pituitary images, cell density was measured by counting the number of haematoxylin positive nuclei per 35mm^2 and pituitary volume was measured using ImageJ. TSH^{+ve} cell volume was measured using Volocity. Immunostained *Sox3*$^{+/\Delta GFP}$ neurospheres are imaged and quantified according to the number of SOX3 and GFP positive cells they contain. The spheres are categorized into mainly SOX3^{+ve} spheres or mainly GFP^{+ve} spheres. Experiments are carried out at least in triplicate and at least three different fields were quantified for each experiment. For BrdU quantification, only BrdU^{+ve} cells 100µm either side of the 3rd ventricle and within the median eminence were counted. For statistical calculation, angular transformation was performed on percentage values. Unpaired t-test with Welch's correction and two-way ANOVA were used for the analysis of statistical significance and error bars represent the standard deviation.

bioRxiv preprint doi: https://doi.org/10.1101/2023.07.26.550616; this version posted July 28, 2023. The copyright holder for this preprint (which was not certified by peer review) is the author/funder, who has granted bioRxiv a license to display the preprint in perpetuity. It is made available under aCC-BY 4.0 International license.

Author contributions

KR and RLB conceived the project. KR and CG designed the research studies. CG conducted experiments, acquired and analyzed the data. CG, KR and RLB wrote the manuscript.

bioRxiv preprint doi: https://doi.org/10.1101/2023.07.26.550616; this version posted July 28, 2023. The copyright holder for this preprint (which was not certified by peer review) is the author/funder, who has granted bioRxiv a license to display the preprint in perpetuity. It is made available under aCC-BY 4.0 International license.

Acknowledgements

We are grateful for the help and support of all recent past and present members of the Lovell-Badge lab. We are indebted to Dr. AF Parlow and the NHPP for reagents for the RIA and immunofluorescence experiments. We thank Simon Rhodes (Indiana University School of Medicine) for the generous gift of POU1F1 antibodies, J.P. Martinez-Barbera (University College London, UK) for *Ghrh* and *Sst* probes and S. Blackshaw for *Rax* probe. We thank Patrice Mollard (IGF, Montpellier, France) foir helpful discussions. We also thank Biological Services, the light microscopy, the experimental histopathology and the electron microscopy platforms at the MRC National Institute for Medical Research and the Francis Crick Institute, for their excellent assistance and technical support and BioRender for graphical representation.

This work was supported by the Medical Research Council, U.K. (U117512772, U117562207 and U117570590) and by the Francis Crick Institute which receives its core funding from Cancer Research UK (CC2116), the UK Medical Research Council (CC2116), and the Wellcome Trust (CC2116). For the purpose of Open Access, the author has applied a CC BY public copyright licence to any Author Accepted Manuscript version arising from this submission.

bioRxiv preprint doi: https://doi.org/10.1101/2023.07.26.550616; this version posted July 28, 2023. The copyright holder for this preprint (which was not certified by peer review) is the author/funder, who has granted bioRxiv a license to display the preprint in perpetuity. It is made available under aCC-BY 4.0 International license.

Reference

1. Burbridge S, Stewart I, and Placzek M. Development of the Neuroendocrine Hypothalamus. *Compr Physiol.* 2016;6(2):623-43.
2. Rizzoti K, and Lovell-Badge R. Pivotal role of median eminence tanycytes for hypothalamic function and neurogenesis. *Mol Cell Endocrinol.* 2017;445:7-13.
3. Clayton RW, Lovell-Badge R, and Galichet C. The Properties and Functions of Glial Cell Types of the Hypothalamic Median Eminence. *Front Endocrinol (Lausanne).* 2022;13:953995.
4. Djogo T, Robins SC, Schneider S, Kryzskaya D, Liu X, Mingay A, et al. Adult NG2-Glia Are Required for Median Eminence-Mediated Leptin Sensing and Body Weight Control. *Cell Metab.* 2016;23(5):797-810.
5. Buller S, Kohnke S, Hansford R, Shimizu T, Richardson WD, and Blouet C. Median eminence myelin continuously turns over in adult mice. *Mol Metab.* 2023;69:101690.
6. Kohnke S, Buller S, Nuzzaci D, Ridley K, Lam B, Pivonkova H, et al. Nutritional regulation of oligodendrocyte differentiation regulates perineuronal net remodeling in the median eminence. *Cell Rep.* 2021;36(2):109362.
7. Galichet C, Clayton RW, and Lovell-Badge R. Novel Tools and Investigative Approaches for the Study of Oligodendrocyte Precursor Cells (NG2-Glia) in CNS Development and Disease. *Front Cell Neurosci.* 2021;15:673132.

bioRxiv preprint doi: https://doi.org/10.1101/2023.07.26.550616; this version posted July 28, 2023. The copyright holder for this preprint (which was not certified by peer review) is the author/funder, who has granted bioRxiv a license to display the preprint in perpetuity. It is made available under aCC-BY 4.0 International license.

8. Prevot V, Dehouck B, Sharif A, Ciofi P, Giacobini P, and Clasadonte J. The Versatile Tanycyte: A Hypothalamic Integrator of Reproduction and Energy Metabolism. *Endocr Rev.* 2018;39(3):333-68.

9. Mullier A, Bouret SG, Prevot V, and Dehouck B. Differential distribution of tight junction proteins suggests a role for tanycytes in blood-hypothalamus barrier regulation in the adult mouse brain. *J Comp Neurol.* 2010;518(7):943-62.

10. Rosso L, and Mienville JM. Pituicyte modulation of neurohormone output. *Glia.* 2009;57(3):235-43.

11. Prevot V, Bellefontaine N, Baroncini M, Sharif A, Hanchate NK, Parkash J, et al. Gonadotrophin-releasing hormone nerve terminals, tanycytes and neurohaemal junction remodelling in the adult median eminence: functional consequences for reproduction and dynamic role of vascular endothelial cells. *J Neuroendocrinol.* 2010;22(7):639-49.

12. Joseph-Bravo P, Jaimes-Hoy L, Uribe RM, and Charli JL. 60 YEARS OF NEUROENDOCRINOLOGY: TRH, the first hypophysiotropic releasing hormone isolated: control of the pituitary-thyroid axis. *J Endocrinol.* 2015;226(2):T85-T100.

13. Balland E, Dam J, Langlet F, Caron E, Steculorum S, Messina A, et al. Hypothalamic tanycytes are an ERK-gated conduit for leptin into the brain. *Cell Metab.* 2014;19(2):293-301.

14. Bolborea M, and Dale N. Hypothalamic tanycytes: potential roles in the control of feeding and energy balance. *Trends Neurosci.* 2013;36(2):91-100.

15. Sharif A, Fitzsimons CP, and Lucassen PJ. Neurogenesis in the adult hypothalamus: A distinct form of structural plasticity involved in metabolic and

bioRxiv preprint doi: https://doi.org/10.1101/2023.07.26.550616; this version posted July 28, 2023. The copyright holder for this preprint (which was not certified by peer review) is the author/funder, who has granted bioRxiv a license to display the preprint in perpetuity. It is made available under aCC-BY 4.0 International license.

circadian regulation, with potential relevance for human pathophysiology. *Handb Clin Neurol.* 2021;179:125-40.

16. Lee DA, Bedont JL, Pak T, Wang H, Song J, Miranda-Angulo A, et al. Tanycytes of the hypothalamic median eminence form a diet-responsive neurogenic niche. *Nat Neurosci.* 2012;15(5):700-2.

17. Li J, Tang Y, and Cai D. IKKbeta/NF-kappaB disrupts adult hypothalamic neural stem cells to mediate a neurodegenerative mechanism of dietary obesity and pre-diabetes. *Nat Cell Biol.* 2012;14(10):999-1012.

18. Haan N, Goodman T, Najdi-Samiei A, Stratford CM, Rice R, El Agha E, et al. Fgf10-expressing tanycytes add new neurons to the appetite/energy-balance regulating centers of the postnatal and adult hypothalamus. *J Neurosci.* 2013;33(14):6170-80.

19. Robins SC, Stewart I, McNay DE, Taylor V, Giachino C, Goetz M, et al. alpha-Tanycytes of the adult hypothalamic third ventricle include distinct populations of FGF-responsive neural progenitors. *Nat Commun.* 2013;4:2049.

20. Furube E, Ishii H, Nambu Y, Kurganov E, Nagaoka S, Morita M, et al. Neural stem cell phenotype of tanycyte-like ependymal cells in the circumventricular organs and central canal of adult mouse brain. *Sci Rep.* 2020;10(1):2826.

21. Sarkar A, and Hochedlinger K. The sox family of transcription factors: versatile regulators of stem and progenitor cell fate. *Cell Stem Cell.* 2013;12(1):15-30.

22. Wood HB, and Episkopou V. Comparative expression of the mouse Sox1, Sox2 and Sox3 genes from pre-gastrulation to early somite stages. *Mech Dev.* 1999;86(1-2):197-201.

bioRxiv preprint doi: https://doi.org/10.1101/2023.07.26.550616; this version posted July 28, 2023. The copyright holder for this preprint (which was not certified by peer review) is the author/funder, who has granted bioRxiv a license to display the preprint in perpetuity. It is made available under aCC-BY 4.0 International license.

23. Bylund M, Andersson E, Novitch BG, and Muhr J. Vertebrate neurogenesis is counteracted by Sox1-3 activity. *Nat Neurosci.* 2003;6(11):1162-8.

24. Hoffmann SA, Hos D, Kuspert M, Lang RA, Lovell-Badge R, Wegner M, et al. Stem cell factor Sox2 and its close relative Sox3 have differentiation functions in oligodendrocytes. *Development.* 2014;141(1):39-50.

25. Kelberman D, Rizzoti K, Lovell-Badge R, Robinson IC, and Dattani MT. Genetic regulation of pituitary gland development in human and mouse. *Endocr Rev.* 2009;30(7):790-829.

26. Rizzoti K, Brunelli S, Carmignac D, Thomas PQ, Robinson IC, and Lovell-Badge R. SOX3 is required during the formation of the hypothalamo-pituitary axis. *Nat Genet.* 2004;36(3):247-55.

27. Huang N, Chen D, Wu X, Chen X, Zhang X, Niu J, et al. Aspirin Promotes Oligodendroglial Differentiation Through Inhibition of Wnt Signaling Pathway. *Mol Neurobiol.* 2016;53(5):3258-66.

28. Chen J, Zuo S, Wang J, Huang J, Zhang X, Liu Y, et al. Aspirin promotes oligodendrocyte precursor cell proliferation and differentiation after white matter lesion. *Front Aging Neurosci.* 2014;6:7.

29. Rogers N, Cheah PS, Szarek E, Banerjee K, Schwartz J, and Thomas P. Expression of the murine transcription factor SOX3 during embryonic and adult neurogenesis. *Gene Expr Patterns.* 2013;13(7):240-8.

30. Isaka F, Ishibashi M, Taki W, Hashimoto N, Nakanishi S, and Kageyama R. Ectopic expression of the bHLH gene Math1 disturbs neural development. *Eur J Neurosci.* 1999;11(7):2582-8.

bioRxiv preprint doi: https://doi.org/10.1101/2023.07.26.550616; this version posted July 28, 2023. The copyright holder for this preprint (which was not certified by peer review) is the author/funder, who has granted bioRxiv a license to display the preprint in perpetuity. It is made available under aCC-BY 4.0 International license.

31. Cheung L, Le Tissier P, Goldsmith SG, Treier M, Lovell-Badge R, and Rizzoti K. NOTCH activity differentially affects alternative cell fate acquisition and maintenance. *Elife.* 2018;7.

32. Galichet C, Lovell-Badge R, and Rizzoti K. Nestin-Cre mice are affected by hypopituitarism, which is not due to significant activity of the transgene in the pituitary gland. *PLoS One.* 2010;5(7):e11443.

33. Hu Z, Friberg RD, and Barkan AL. Ontogeny of GH mRNA and GH secretion in male and female rats: regulation by GH-releasing hormone. *Am J Physiol.* 1993;265(2 Pt 1):E236-42.

34. Khetchoumian K, Balsalobre A, Mayran A, Christian H, Chenard V, St-Pierre J, et al. Pituitary cell translation and secretory capacities are enhanced cell autonomously by the transcription factor Creb3l2. *Nat Commun.* 2019;10(1):3960.

35. Melmed S. Pathogenesis of pituitary tumors. *Nat Rev Endocrinol.* 2011;7(5):257-66.

36. Salvatierra J, Lee DA, Zibetti C, Duran-Moreno M, Yoo S, Newman EA, et al. The LIM homeodomain factor Lhx2 is required for hypothalamic tanycyte specification and differentiation. *J Neurosci.* 2014;34(50):16809-20.

37. McNay DE, Briancon N, Kokoeva MV, Maratos-Flier E, and Flier JS. Remodeling of the arcuate nucleus energy-balance circuit is inhibited in obese mice. *J Clin Invest.* 2012;122(1):142-52.

38. Nesan D, Thornton HF, Sewell LC, and Kurrasch DM. An Efficient Method for Generating Murine Hypothalamic Neurospheres for the Study of Regional Neural Progenitor Biology. *Endocrinology.* 2020;161(4).

bioRxiv preprint doi: https://doi.org/10.1101/2023.07.26.550616; this version posted July 28, 2023. The copyright holder for this preprint (which was not certified by peer review) is the author/funder, who has granted bioRxiv a license to display the preprint in perpetuity. It is made available under aCC-BY 4.0 International license.

39. Conti L, and Cattaneo E. Neural stem cell systems: physiological players or in vitro entities? *Nat Rev Neurosci.* 2010;11(3):176-87.

40. Llorente V, Velarde P, Desco M, and Gomez-Gaviro MV. Current Understanding of the Neural Stem Cell Niches. *Cells.* 2022;11(19).

41. Wang TW, Stromberg GP, Whitney JT, Brower NW, Klymkowsky MW, and Parent JM. Sox3 expression identifies neural progenitors in persistent neonatal and adult mouse forebrain germinative zones. *J Comp Neurol.* 2006;497(1):88-100.

42. Rojczyk-Golebiewska E, Palasz A, and Wiaderkiewicz R. Hypothalamic subependymal niche: a novel site of the adult neurogenesis. *Cell Mol Neurobiol.* 2014;34(5):631-42.

43. Robins SC, and Kokoeva MV. NG2-Glia, a New Player in Energy Balance. *Neuroendocrinology.* 2018;107(3):305-12.

44. Rizzoti K, and Lovell-Badge R. SOX3 activity during pharyngeal segmentation is required for craniofacial morphogenesis. *Development.* 2007;134(19):3437-48.

45. Asadi A, Shadab Mehr N, Mohamadi MH, Shokri F, Heidary M, Sadeghifard N, et al. Obesity and gut-microbiota-brain axis: A narrative review. *J Clin Lab Anal.* 2022;36(5):e24420.

46. Qi M, Tan B, Wang J, Liao S, Deng Y, Ji P, et al. The microbiota-gut-brain axis: A novel nutritional therapeutic target for growth retardation. *Crit Rev Food Sci Nutr.* 2022;62(18):4867-92.

47. Yu KB, and Hsiao EY. Roles for the gut microbiota in regulating neuronal feeding circuits. *J Clin Invest.* 2021;131(10).

bioRxiv preprint doi: https://doi.org/10.1101/2023.07.26.550616; this version posted July 28, 2023. The copyright holder for this preprint (which was not certified by peer review) is the author/funder, who has granted bioRxiv a license to display the preprint in perpetuity. It is made available under aCC-BY 4.0 International license.

48. Bando H, Urai S, Kanie K, Sasaki Y, Yamamoto M, Fukuoka H, et al. Novel genes and variants associated with congenital pituitary hormone deficiency in the era of next-generation sequencing. *Front Endocrinol (Lausanne).* 2022;13:1008306.

49. Parkin K, Kapoor R, Bhat R, and Greenough A. Genetic causes of hypopituitarism. *Arch Med Sci.* 2020;16(1):27-33.

50. Fang Q, George AS, Brinkmeier ML, Mortensen AH, Gergics P, Cheung LY, et al. Genetics of Combined Pituitary Hormone Deficiency: Roadmap into the Genome Era. *Endocr Rev.* 2016;37(6):636-75.

51. Lamperti A, and Mastovich J. Morphological changes in the hypothalamic arcuate nucleus and median eminence in the golden hamster during the neonatal period. *Am J Anat.* 1983;166(2):173-85.

52. Pastor FE, Blazquez JL, Toranzo D, Pelaez B, Sanchez A, Alvarez-Morujo AJ, et al. Myelinated Herring bodies in the median eminence of the cat. *Histol Histopathol.* 1991;6(2):161-5.

53. Rutzel H, and Schiebler TH. Prenatal and early postnatal development of the glial cells in the median eminence of the rat. *Cell Tissue Res.* 1980;211(1):117-37.

54. Silverman AJ, and Desnoyers P. Post-natal development of the median eminence of the guinea pig. *Anat Rec.* 1975;183(3):459-75.

55. Mirzadeh Z, Alonge KM, Cabrales E, Herranz-Perez V, Scarlett JM, Brown JM, et al. Perineuronal Net Formation during the Critical Period for Neuronal Maturation in the Hypothalamic Arcuate Nucleus. *Nat Metab.* 2019;1(2):212-21.

bioRxiv preprint doi: https://doi.org/10.1101/2023.07.26.550616; this version posted July 28, 2023. The copyright holder for this preprint (which was not certified by peer review) is the author/funder, who has granted bioRxiv a license to display the preprint in perpetuity. It is made available under aCC-BY 4.0 International license.

56. Bartkowska K, Turlejski K, Koguc-Sobolewska P, and Djavadian R. Adult Neurogenesis in the Mammalian Hypothalamus: Impact of Newly Generated Neurons on Hypothalamic Function. *Neuroscience.* 2023;515:83-92.

57. Ost'adalova I, and Babicky A. Periodization of the early postnatal development in the rat with particular attention to the weaning period. *Physiol Res.* 2012;61(Suppl 1):S1-7.

58. Richter SH, Kastner N, Loddenkemper DH, Kaiser S, and Sachser N. A Time to Wean? Impact of Weaning Age on Anxiety-Like Behaviour and Stability of Behavioural Traits in Full Adulthood. *PLoS One.* 2016;11(12):e0167652.

59. Schwartz MW, Woods SC, Porte D, Jr., Seeley RJ, and Baskin DG. Central nervous system control of food intake. *Nature.* 2000;404(6778):661-71.

60. Anthwal N, Pelling M, Claxton S, Mellitzer G, Collin C, Kessaris N, et al. Conditional deletion of neurogenin-3 using Nkx2.1iCre results in a mouse model for the central control of feeding, activity and obesity. *Dis Model Mech.* 2013;6(5):1133-45.

61. White AK, Drake KD, Porczak AE, Tirado-Mansilla G, Lee MF, Hyatt KC, et al. Integrity of the minor spliceosome in the developing mouse hypothalamus determines neuronal subtype composition regulating energy balance. *bioRxiv.* 2022:2022.10.04.510883.

62. Stolovich-Rain M, Enk J, Vikesa J, Nielsen FC, Saada A, Glaser B, et al. Weaning triggers a maturation step of pancreatic beta cells. *Dev Cell.* 2015;32(5):535-45.

bioRxiv preprint doi: https://doi.org/10.1101/2023.07.26.550616; this version posted July 28, 2023. The copyright holder for this preprint (which was not certified by peer review) is the author/funder, who has granted bioRxiv a license to display the preprint in perpetuity. It is made available under aCC-BY 4.0 International license.

63. Favaro R, Valotta M, Ferri AL, Latorre E, Mariani J, Giachino C, et al. Hippocampal development and neural stem cell maintenance require Sox2-dependent regulation of Shh. *Nat Neurosci.* 2009;12(10):1248-56.

64. Kan L, Israsena N, Zhang Z, Hu M, Zhao LR, Jalali A, et al. Sox1 acts through multiple independent pathways to promote neurogenesis. *Dev Biol.* 2004;269(2):580-94.

65. Kan L, Jalali A, Zhao LR, Zhou X, McGuire T, Kazanis I, et al. Dual function of Sox1 in telencephalic progenitor cells. *Dev Biol.* 2007;310(1):85-98.

66. Radecki DZ, and Samanta J. Endogenous Neural Stem Cell Mediated Oligodendrogenesis in the Adult Mammalian Brain. *Cells.* 2022;11(13).

67. Appelman-Dijkstra NM, Kokshoorn NE, Dekkers OM, Neelis KJ, Biermasz NR, Romijn JA, et al. Pituitary dysfunction in adult patients after cranial radiotherapy: systematic review and meta-analysis. *J Clin Endocrinol Metab.* 2011;96(8):2330-40.

68. Forbes ME, Paitsel M, Bourland JD, and Riddle DR. Systemic effects of fractionated, whole-brain irradiation in young adult and aging rats. *Radiat Res.* 2013;180(3):326-33.

69. Ornelas A, Zacharias-Millward N, Menter DG, Davis JS, Lichtenberger L, Hawke D, et al. Beyond COX-1: the effects of aspirin on platelet biology and potential mechanisms of chemoprevention. *Cancer Metastasis Rev.* 2017;36(2):289-303.

70. Hoozemans JJ, Rozemuller AJ, Janssen I, De Groot CJ, Veerhuis R, and Eikelenboom P. Cyclooxygenase expression in microglia and neurons in Alzheimer's disease and control brain. *Acta Neuropathol.* 2001;101(1):2-8.

bioRxiv preprint doi: https://doi.org/10.1101/2023.07.26.550616; this version posted July 28, 2023. The copyright holder for this preprint (which was not certified by peer review) is the author/funder, who has granted bioRxiv a license to display the preprint in perpetuity. It is made available under aCC-BY 4.0 International license.

71. de Seranno S, d'Anglemont de Tassigny X, Estrella C, Loyens A, Kasparov S, Leroy D, et al. Role of estradiol in the dynamic control of tanycyte plasticity mediated by vascular endothelial cells in the median eminence. *Endocrinology.* 2010;151(4):1760-72.

72. Dovizio M, Tacconelli S, Sostres C, Ricciotti E, and Patrignani P. Mechanistic and pharmacological issues of aspirin as an anticancer agent. *Pharmaceuticals (Basel).* 2012;5(12):1346-71.

73. Morais LH, Schreiber HLt, and Mazmanian SK. The gut microbiota-brain axis in behaviour and brain disorders. *Nat Rev Microbiol.* 2021;19(4):241-55.

74. Lu J, Lu L, Yu Y, Cluette-Brown J, Martin CR, and Claud EC. Effects of Intestinal Microbiota on Brain Development in Humanized Gnotobiotic Mice. *Sci Rep.* 2018;8(1):5443.

75. Lu J, Synowiec S, Lu L, Yu Y, Bretherick T, Takada S, et al. Microbiota influence the development of the brain and behaviors in C57BL/6J mice. *PLoS One.* 2018;13(8):e0201829.

76. Sudo N, Chida Y, Aiba Y, Sonoda J, Oyama N, Yu XN, et al. Postnatal microbial colonization programs the hypothalamic-pituitary-adrenal system for stress response in mice. *J Physiol.* 2004;558(Pt 1):263-75.

77. Schloss PD, Schubert AM, Zackular JP, Iverson KD, Young VB, and Petrosino JF. Stabilization of the murine gut microbiome following weaning. *Gut Microbes.* 2012;3(4):383-93.

bioRxiv preprint doi: https://doi.org/10.1101/2023.07.26.550616; this version posted July 28, 2023. The copyright holder for this preprint (which was not certified by peer review) is the author/funder, who has granted bioRxiv a license to display the preprint in perpetuity. It is made available under aCC-BY 4.0 International license.

78. Al Nabhani Z, Dulauroy S, Marques R, Cousu C, Al Bounny S, Dejardin F, et al. A Weaning Reaction to Microbiota Is Required for Resistance to Immunopathologies in the Adult. *Immunity.* 2019;50(5):1276-88 e5.

79. Gabanyi I, Lepousez G, Wheeler R, Vieites-Prado A, Nissant A, Chevalier G, et al. Bacterial sensing via neuronal Nod2 regulates appetite and body temperature. *Science.* 2022;376(6590):eabj3986.

80. Girardin SE, Travassos LH, Herve M, Blanot D, Boneca IG, Philpott DJ, et al. Peptidoglycan molecular requirements allowing detection by Nod1 and Nod2. *J Biol Chem.* 2003;278(43):41702-8.

81. Vesth T, Ozen A, Andersen SC, Kaas RS, Lukjancenko O, Bohlin J, et al. Veillonella, Firmicutes: Microbes disguised as Gram negatives. *Stand Genomic Sci.* 2013;9(2):431-48.

82. Wexler HM. Bacteroides: the good, the bad, and the nitty-gritty. *Clin Microbiol Rev.* 2007;20(4):593-621.

83. Rivers LE, Young KM, Rizzi M, Jamen F, Psachoulia K, Wade A, et al. PDGFRA/NG2 glia generate myelinating oligodendrocytes and piriform projection neurons in adult mice. *Nat Neurosci.* 2008;11(12):1392-401.

84. Srinivas S, Watanabe T, Lin CS, William CM, Tanabe Y, Jessell TM, et al. Cre reporter strains produced by targeted insertion of EYFP and ECFP into the ROSA26 locus. *BMC Dev Biol.* 2001;1:4.

85. McGuinness L, Magoulas C, Sesay AK, Mathers K, Carmignac D, Manneville JB, et al. Autosomal dominant growth hormone deficiency disrupts secretory vesicles in vitro and in vivo in transgenic mice. *Endocrinology.* 2003;144(2):720-31.

bioRxiv preprint doi: https://doi.org/10.1101/2023.07.26.550616; this version posted July 28, 2023. The copyright holder for this preprint (which was not certified by peer review) is the author/funder, who has granted bioRxiv a license to display the preprint in perpetuity. It is made available under aCC-BY 4.0 International license.

86. Scott CE, Wynn SL, Sesay A, Cruz C, Cheung M, Gomez Gaviro MV, et al. SOX9 induces and maintains neural stem cells. *Nat Neurosci.* 2010;13(10):1181-9.

87. Ozen I, Galichet C, Watts C, Parras C, Guillemot F, and Raineteau O. Proliferating neuronal progenitors in the postnatal hippocampus transiently express the proneural gene Ngn2. *Eur J Neurosci.* 2007;25(9):2591-603.

88. Furukawa T, Kozak CA, and Cepko CL. rax, a novel paired-type homeobox gene, shows expression in the anterior neural fold and developing retina. *Proc Natl Acad Sci U S A.* 1997;94(7):3088-93.

89. Livak KJ, and Schmittgen TD. Analysis of relative gene expression data using real-time quantitative PCR and the 2(-Delta Delta C(T)) Method. *Methods.* 2001;25(4):402-8.

bioRxiv preprint doi: https://doi.org/10.1101/2023.07.26.550616; this version posted July 28, 2023. The copyright holder for this preprint (which was not certified by peer review) is the author/funder, who has granted bioRxiv a license to display the preprint in perpetuity. It is made available under aCC-BY 4.0 International license.

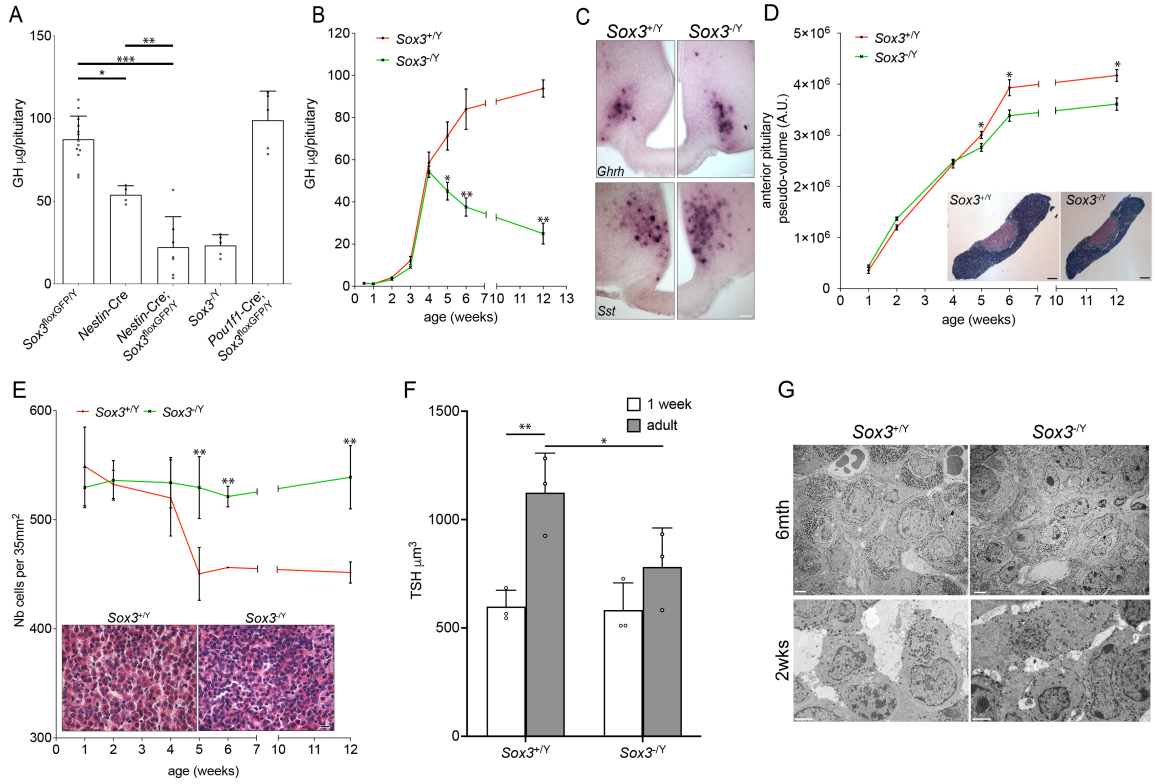

Figure 1: The hypopituitarism in *Sox3*-null mutants has a hypothalamic origin and develops after weaning, concomitantly with defective pituitary endocrine cell maturation

(A) GH contents of 2-month *Sox3*$^{floxGFP/Y}$, *Nestin*-Cre, *Nestin*-Cre; *Sox3*$^{floxGFP/Y}$, *Sox3*$^{-/Y}$ and *Pit1*-Cre; *Sox3*$^{floxGFP/Y}$ pituitaries. Reduction in GH contents only appears when SOX3 is removed from the CNS. (B) GH contents of *Sox3*$^{+/Y}$ and *Sox3*$^{-/Y}$ at different post-natal weeks. Reduction in GH contents in *Sox3*-null animals appears post-weaning. (C) *In situ* hybridization for *Ghrh* (upper panels) and *somatostatin* (*Sst*, lower panels) on 2-month *Sox3*$^{+/Y}$ and *Sox3*$^{-/Y}$ hypothalami. Scale bar: 100µm. (D) *Sox3*$^{+/Y}$ and *Sox3*$^{-/Y}$ anterior pituitary sizes at different post-natal weeks. Insets represent 2-month control and *Sox3*-null H&E-stained pituitaries. *Sox3*-null anterior pituitaries are smaller post-weaning. Scale bar: 200µm. (E) *Sox3*$^{+/Y}$ and *Sox3*$^{-/Y}$ anterior pituitary cell densities. Insets represent 2-month control and *Sox3*-null H&E-stained anterior pituitaries. *Sox3*-null anterior pituitary cell densities remain constant while these decrease in controls post-weaning. Scale bar: 15µm. (F) *Sox3*$^{+/Y}$ and *Sox3*$^{-/Y}$ TSH^{+ve} cell volumes at 1 week (white columns) and 2 months (grey columns). TSH^{+ve} cell volumes increase with age in controls and remain constant in *Sox3* mutants. (G) Transmission electron microscopy images of 2-week and 6-month control and *Sox3*$^{-/Y}$ anterior pituitaries. Fewer secretory granules are present in 6-month *Sox3*-null anterior pituitaries. Scale bar: 2µm.

*: $p<0.05$; **: $p<0.01$; ***: $p<0.001$

bioRxiv preprint doi: https://doi.org/10.1101/2023.07.26.550616; this version posted July 28, 2023. The copyright holder for this preprint (which was not certified by peer review) is the author/funder, who has granted bioRxiv a license to display the preprint in perpetuity. It is made available under aCC-BY 4.0 International license.

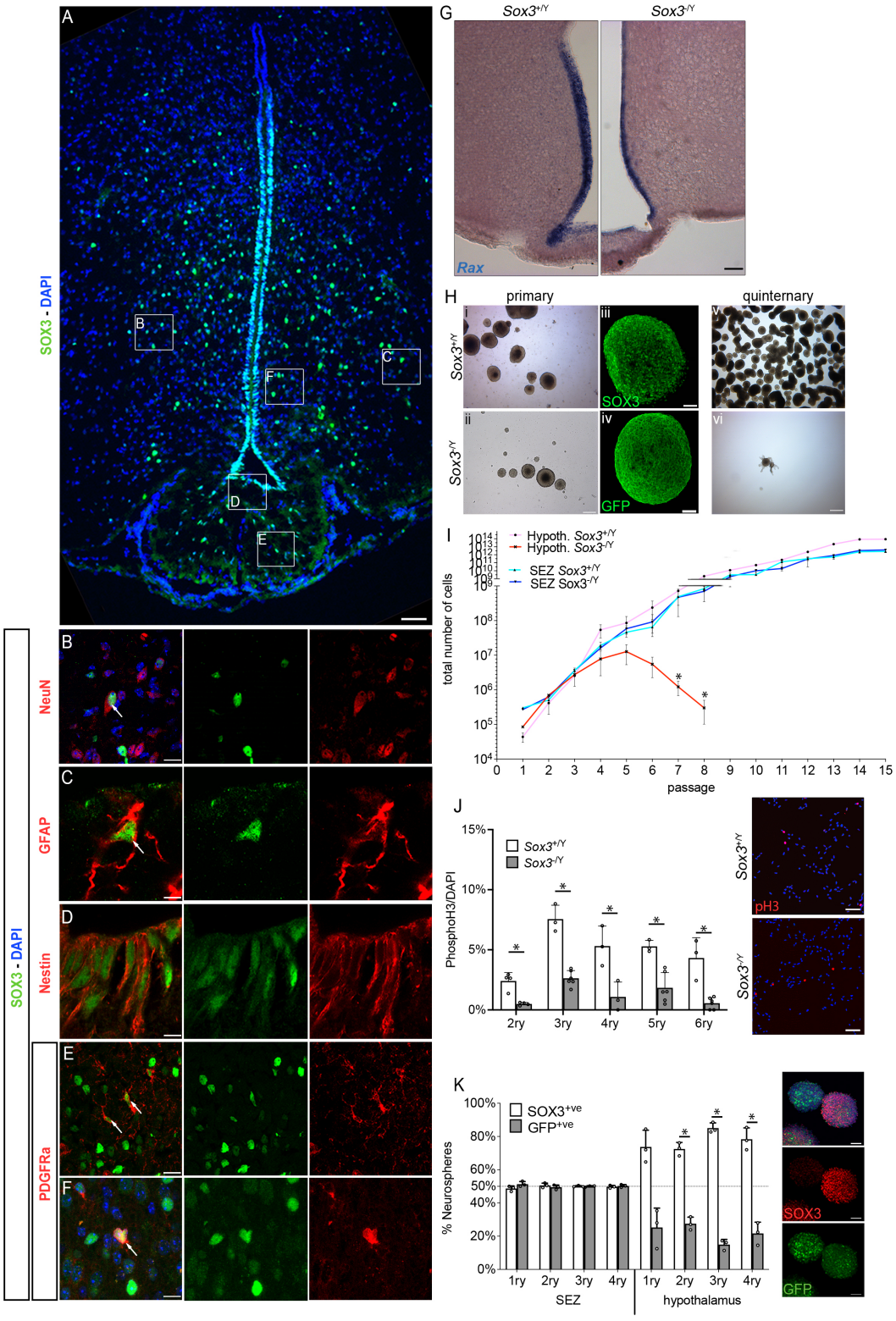

Figure 2: SOX3 is expressed in hypothalamic SCs and NG2-glia, and it is required for hypothalamic neurosphere maintenance

bioRxiv preprint doi: https://doi.org/10.1101/2023.07.26.550616; this version posted July 28, 2023. The copyright holder for this preprint (which was not certified by peer review) is the author/funder, who has granted bioRxiv a license to display the preprint in perpetuity. It is made available under aCC-BY 4.0 International license.

(A- F) Fluorescent immunolabelling for SOX3 alone (A) or together with NeuN (Neurons - B), GFAP (astrocytes - C), Nestin (Tanycyctes - D) or PDGFRa (NG2-glia - E-F) in 2 month-old hypothalami. Arrows point to double positive cells. Scale bar: 100µm (A), 10µm (C, F), 20µm (B, D, E). (G) *In situ* hybridization for *Rax* on 2-month control and *Sox3*$^{-/Y}$ hypothalami. Scale bar: 100µm. (H) *Sox3*$^{+/Y}$ (i, iii, vi) and *Sox3*$^{-/Y}$ (ii, iv, vii) hypothalamic derived neurospheres at primary (i,ii) or quintenary (vi,vii) passage. Scale bar: 200µm (primary) and 400µm (quintenary). Insets show neurospheres immunolabelled for SOX3 (control spheres - iii) or GFP (*Sox3*-null spheres - iv). Scale bar: 50µm. (I) Total number of cells after each passage of hypothalamic derived (red lines) or SEZ derived (blue lines) neural stem cells from *Sox3*$^{+/Y}$ (light colour) or *Sox3*$^{-/Y}$ (dark colour) mice. *Sox3*-null hypothalamic derived neurospheres cannot be maintained in culture. (J) Percentage of mitotic cells in progenitor monolayer culture. Insets represent mitotic cells immunolabelled with phospho-Histone 3. Scale bar: 50 µm. There is a proliferation defect in *Sox3*-null progenitors. (K) Percentage of *Sox3*$^{+/\Delta GFP}$ neurospheres containing mostly SOX3^{+ve} cells (white columns) or mostly GFP^{+ve} cells (grey columns) derived from SEZ or hypothalami. *Sox3*$^{+/\Delta GFP}$ hypothalamic neurospheres are not maintained in culture.
*: $p<0.05$

bioRxiv preprint doi: https://doi.org/10.1101/2023.07.26.550616; this version posted July 28, 2023. The copyright holder for this preprint (which was not certified by peer review) is the author/funder, who has granted bioRxiv a license to display the preprint in perpetuity. It is made available under aCC-BY 4.0 International license.

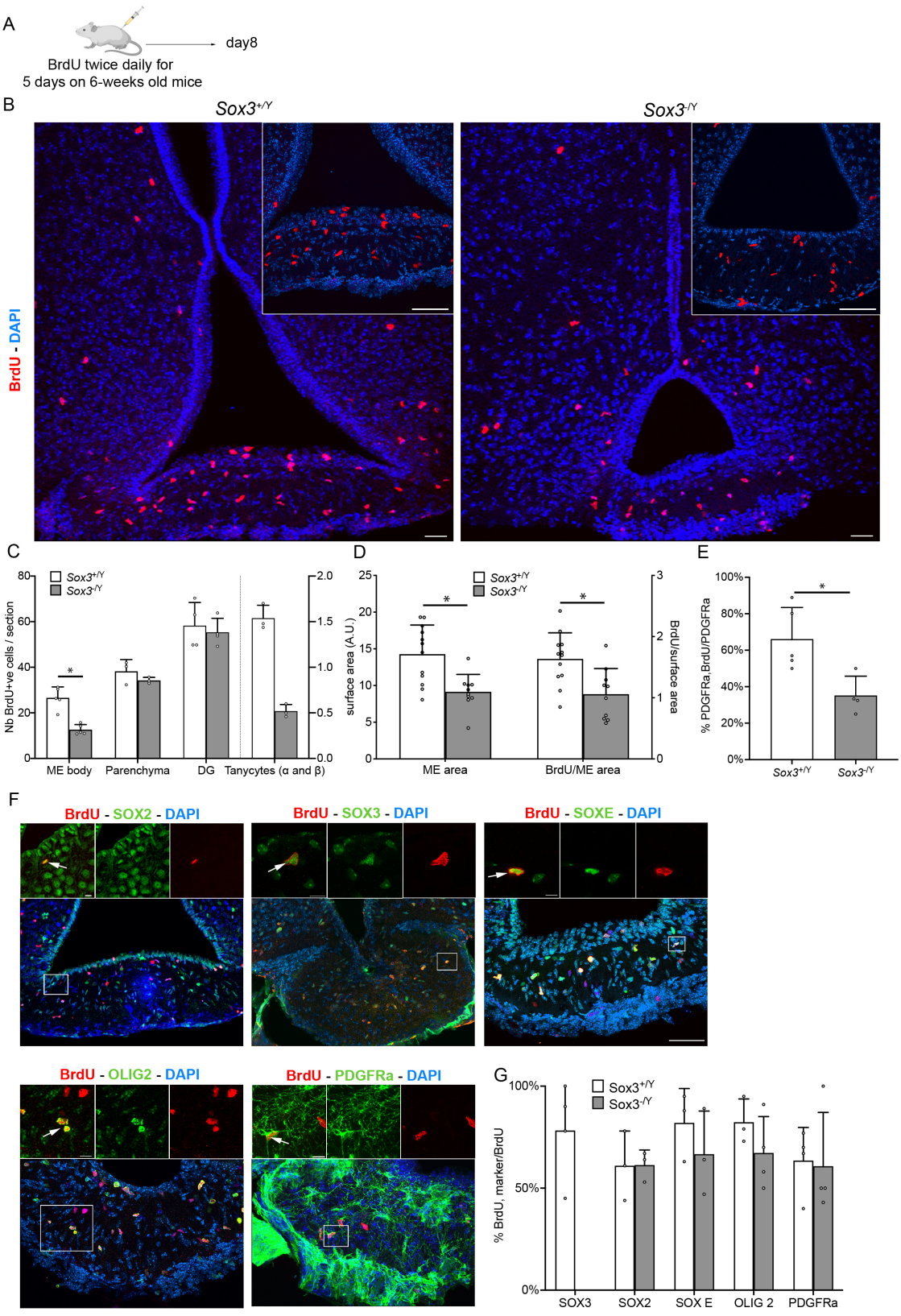

Figure 3: Cell renewal in ME is reduced in absence of SOX3

bioRxiv preprint doi: https://doi.org/10.1101/2023.07.26.550616; this version posted July 28, 2023. The copyright holder for this preprint (which was not certified by peer review) is the author/funder, who has granted bioRxiv a license to display the preprint in perpetuity. It is made available under aCC-BY 4.0 International license.

(A) BrdU administration paradigm. (B) Fluorescent immunolabelling for BrdU on 2-month control and *Sox3*$^{-/Y}$ hypothalami. Insets show ME only. Fewer BrdU^{+ve} cells are present in the *Sox3*$^{-/Y}$ median eminences. Scale bar: 50 µm. (C) Number of BrdU^{+ve} cells in control (white columns) and *Sox3*$^{-/Y}$ (grey columns) median eminences, hypothalamic parenchyma, tanycytes (α and β) and dentate gyri. Fewer BrdU^{+ve} cells are seen in *Sox3*-null median eminences. (D) Median eminence area and BrdU density in control (white columns) and *Sox3*$^{-/Y}$ (grey columns) hypothalami. ME are smaller in *Sox3*-null mice. (E) Percentage of BrdU^{+ve}, PDGFRa^{+ve} NG2-glia in control (white columns) and *Sox3*$^{-/Y}$ (grey columns) median eminences. (F) Fluorescent immunolabelling for BrdU together with SOX2, SOX3, SOX E, OLIG2 or PDGFRa on 2-month control hypothalami. Scale bar: 50 µm. Insets and arrows point to double-positive cells. Scale bar: 10 µm (G) Percentage of BrdU^{+ve} cells expressing either SOX3, SOX2, SOX E, OLIG2, or PDGFRa, in 2-month control (white columns) and *Sox3*$^{-/Y}$ (grey columns) hypothalami. No difference in the identity of BrdU^{+ve} cells between control and *Sox3*-null animals is observed.

*: $p<0.05$

bioRxiv preprint doi: https://doi.org/10.1101/2023.07.26.550616; this version posted July 28, 2023. The copyright holder for this preprint (which was not certified by peer review) is the author/funder, who has granted bioRxiv a license to display the preprint in perpetuity. It is made available under aCC-BY 4.0 International license.

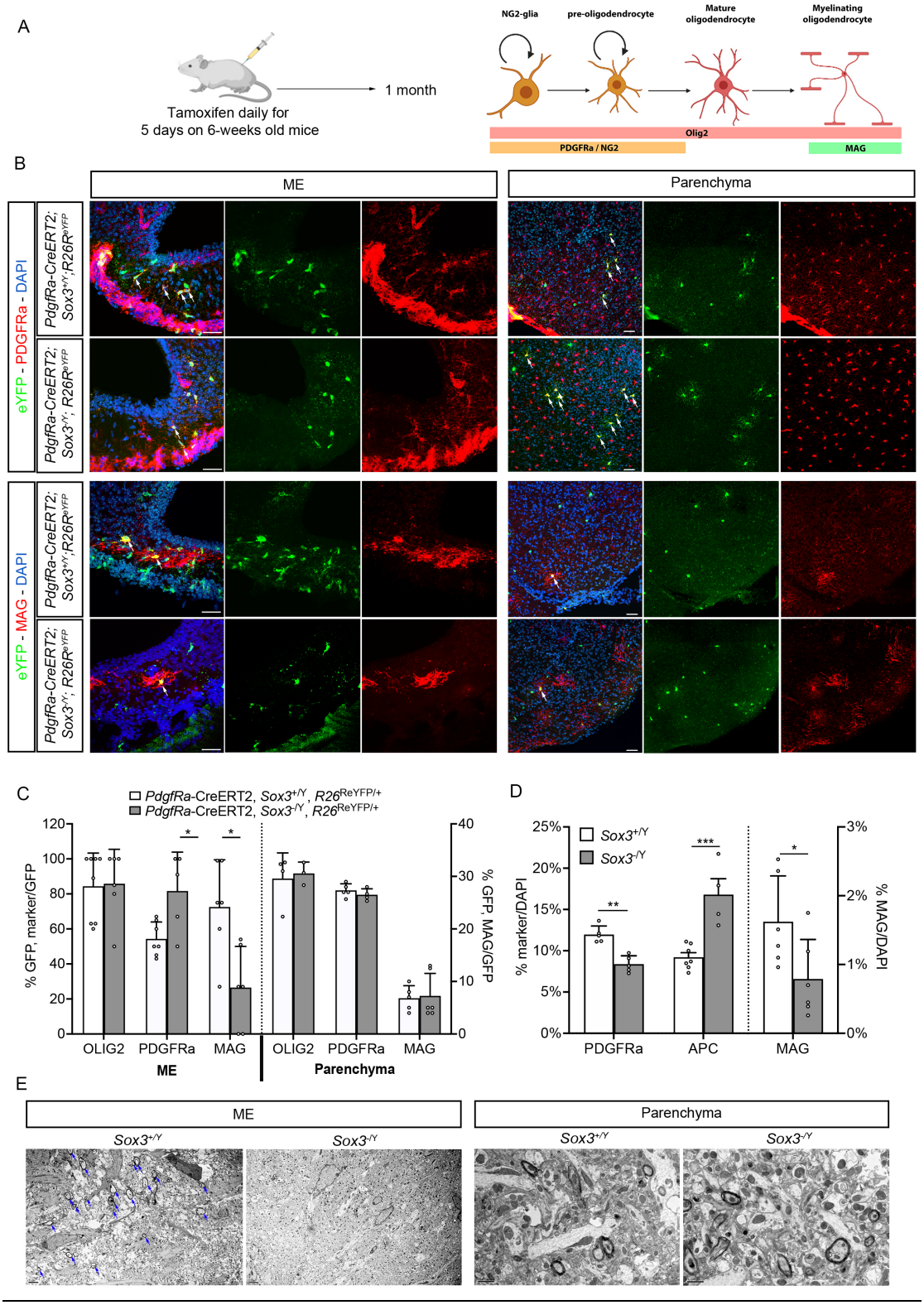

Figure 4: SOX3 loss results in impaired oligodendrocyte differentiation and myelination in ME

bioRxiv preprint doi: https://doi.org/10.1101/2023.07.26.550616; this version posted July 28, 2023. The copyright holder for this preprint (which was not certified by peer review) is the author/funder, who has granted bioRxiv a license to display the preprint in perpetuity. It is made available under aCC-BY 4.0 International license.

(A) Injection paradigm and oligodendrogenesis markers used. (B) Fluorescent Immunolabelling for eYFP and PDGFRa (top panels), MAG (bottom panels) on *Pdgfra*-CreERT2*; Rosa26*$^{ReYFP/+}$; *Sox3*$^{+/Y}$ or *Pdgfra*-CreERT2*; Rosa26*$^{ReYFP/+}$; *Sox3*$^{-/Y}$ hypothalami. Left panels show the ME and the right ones hypothalamic parenchyma. Arrows point to double-positive cells. Scale bar: 50 µm. (C) Percentage of recombinant cells expressing OLIG2, PDGFRa or MAG in ME and parenchyma in *Pdgfra*-CreERT2*; Rosa26*$^{ReYFP/+}$; *Sox3*$^{+/Y}$ (white columns) and *Pdgfra*-CreERT2*; Rosa26*$^{ReYFP/+}$*;Sox3*$^{-/Y}$ (grey columns) hypothalami. Fewer PDGFRa^{+ve} progenitors differentiate into MAG positive cells in *Sox3*-null MEs. (D) Percentage of cells expressing PDGFRa, APC (left Y axis) or MAG (right Y axis) in control (white columns) and *Sox3*-null (grey columns) MEs. There are fewer PDGFRa and MAG present in *Sox3*-null MEs. (E) Transmission electron microscopy images of 2-month *Sox3*$^{+/Y}$ or *Sox3*$^{-/Y}$ MEs (left panels) and hypothalamic parenchymas (right panels). Arrows point to myelinated axons in control ME samples. These are absent in *Sox3* mutant MEs. Scale bars: 2µm for ME and 1µm for Parenchyma.
*: $p<0.05$; **: $p<0.01$; ***: $p<0.001$

bioRxiv preprint doi: https://doi.org/10.1101/2023.07.26.550616; this version posted July 28, 2023. The copyright holder for this preprint (which was not certified by peer review) is the author/funder, who has granted bioRxiv a license to display the preprint in perpetuity. It is made available under aCC-BY 4.0 International license.

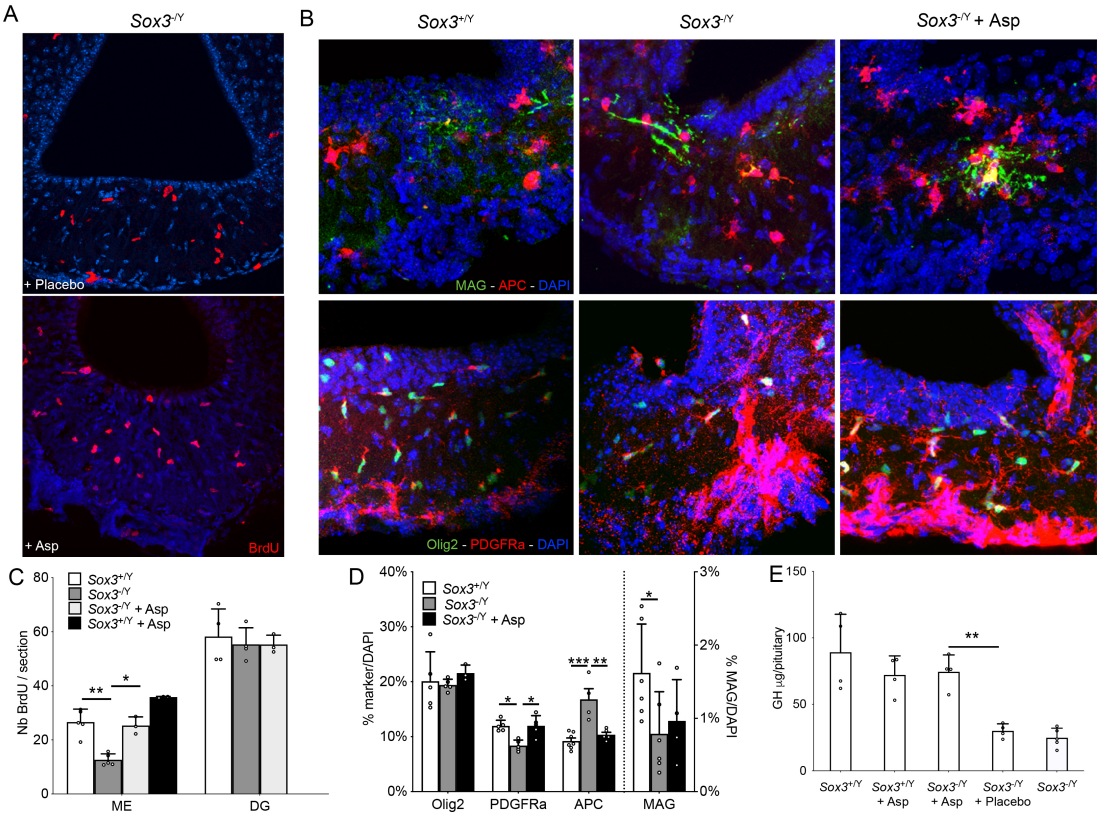

Figure 5: *Sox3*-null NG2 proliferation defect and GH deficiencies are rescued by low dose aspirin treatment.

(A-B) Fluorescent immunolebelling for BrdU on 2-month hypothalami of *Sox3*$^{-/Y}$ mice receiving placebo pellets (top panel) or low dose aspirin pellets (bottom panel) (A) or for OLIG2, PDGFRa and MAG of *Sox3*$^{+/Y}$, *Sox3*$^{-/Y}$ or *Sox3*$^{-/Y}$ receiving low dose aspirin (B). Scale bar: 50 µm for A and 20 µm for B. (C) Number of BrdU^{+ve} cells in the median eminence or dentate gryus of *Sox3*$^{+/Y}$ (white columns), *Sox3*$^{-/Y}$ (dark grey columns), *Sox3*$^{-/Y}$ with low dose aspirin (light grey columns) or *Sox3*$^{+/Y}$ with low dose aspirin (black columns) mice. The number of BrdU^{+ve} cells is rescued in *Sox3*$^{-/Y}$ mice treated with low dose aspirin. (D) Composition of the median eminence in regard to the oligodendrocyte lineage using OLIG2, PDGFRa, APC and MAG of control (white columns), *Sox3*$^{-/Y}$ (grey columns), *Sox3*$^{-/Y}$ with low dose aspirin (black columns) mice. (E) GH contents in 2-month control, control with low dose aspirin, *Sox3*$^{-/Y}$ with low dose aspirin, *Sox3*$^{-/Y}$ with placebo and *Sox3*$^{-/Y}$ pituitaries. GH contents are rescued in *Sox3*-null mice receiving low dose aspirin.
*: p<0.05, **: p<0.01, ***: p<0.001

bioRxiv preprint doi: https://doi.org/10.1101/2023.07.26.550616; this version posted July 28, 2023. The copyright holder for this preprint (which was not certified by peer review) is the author/funder, who has granted bioRxiv a license to display the preprint in perpetuity. It is made available under aCC-BY 4.0 International license.

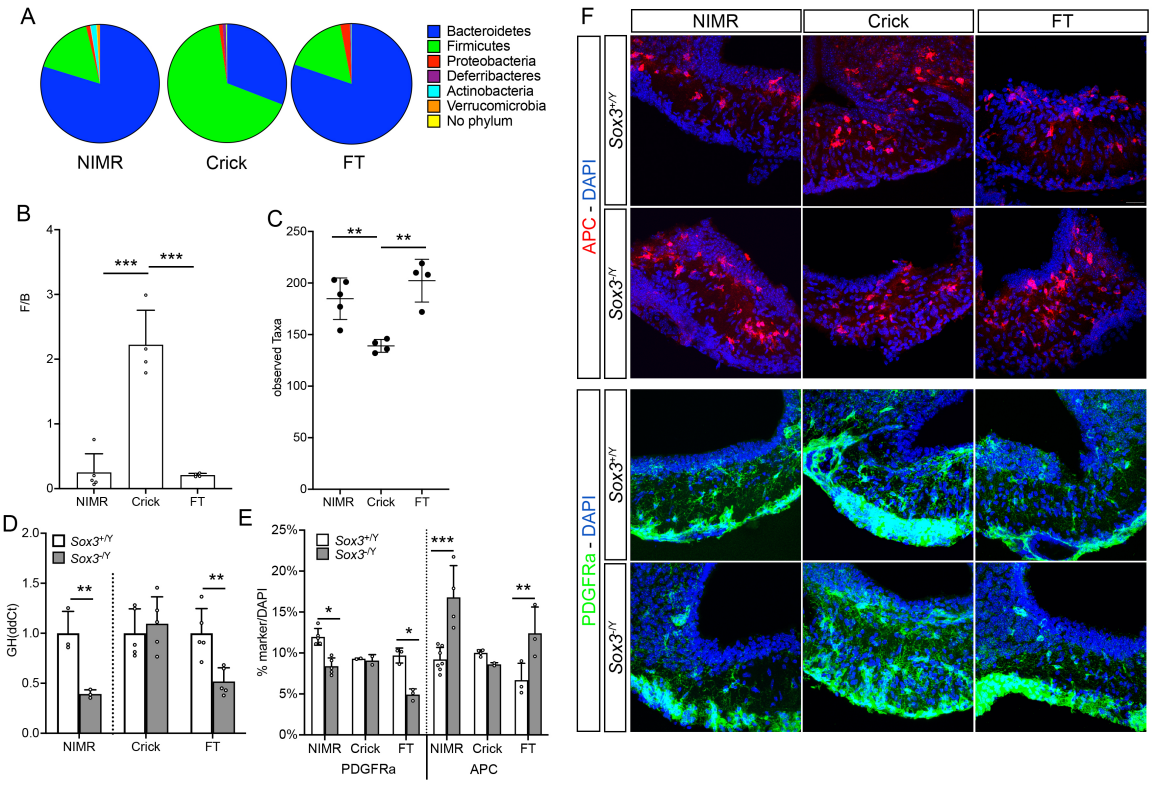

Figure 6: *Sox3*-null NG2-glia ME composition and GH deficiencies is affected by changes of gut microbiota

(A) Abundance of different bacteria phylum in gut microbiota of mice housed at NIMR, Crick or faecal transplanted (FT). (B) Ratio of Firmicutes/Bacteroidetes (F/B) of mice housed at NIMR, Crick or FT. (C) Alpha diversity of the observed taxa species of mice housed at NIMR, Crick or FT. (D) Expression of *Gh* (ddCt) in 2-month NIMR, Crick and FT control (white column) and *Sox3*$^{-/Y}$ (grey columns) pituitaries. (E) Composition of the median eminence in regard to the oligodendrocyte lineage using PDGFRa and APC of NIMR, Crick and FT control (white columns) and *Sox3*$^{-/Y}$ (grey columns) mice. (F) Fluorescent immunolabelling for APC and PDGFRa on 2-month NIMR, Crick and FT control and *Sox3*$^{-/Y}$ hypothalami.
*: $p<0.05$; **: $p<0.01$; ***: $p<0.001$

bioRxiv preprint doi: https://doi.org/10.1101/2023.07.26.550616; this version posted July 28, 2023. The copyright holder for this preprint (which was not certified by peer review) is the author/funder, who has granted bioRxiv a license to display the preprint in perpetuity. It is made available under aCC-BY 4.0 International license.

Antigen	**Host**	**dilution**	**Vendor**
βIII-tubulin	Rabbit	1/100	Abcam
APC	Mouse	1/200	Merck
BrdU	Mouse	1/500	GE life sciences
BrdU	Rat	1/400	Abcam
Nestin	Mouse	1/100	DSHB
GFAP	Mouse	1/1000	Sigma
GFAP	Rabbit	1/1000	Sigma
GFP	Goat	1/200	Abcam
GFP	Rabbit	1/200	Invitrogen
MAG	Rabbit	1/200	NEB
NeuN	Mouse	1/200	Millipore
NG2	Rabbit	1/200	Chemicon
Olig2	Rabbit	1/500	2b scientific
PDGFRa	Goat	1/100	R&D systems
PDGFRa	Rat	1/500	BD Pharmingen
Phospho-histone H3	Mouse	1/500	Abcam
Pit-1	Rabbit	1/1000	gift from Dr Rhodes, Indiana University, USA
Sox2	Rabbit	1/300	Millipore
Sox2	Goat	1/300	ISL
Sox3	Goat	1/100	R&D systems
Sox9	Goat	1/300	R&D systems
SoxE	Rabbit	1/1000	-
TSH	Rabbit	1/100	A.L. Parlow

Table 1: list of primary antibodies used

bioRxiv preprint doi: https://doi.org/10.1101/2023.07.26.550616; this version posted July 28, 2023. The copyright holder for this preprint (which was not certified by peer review) is the author/funder, who has granted bioRxiv a license to display the preprint in perpetuity. It is made available under aCC-BY 4.0 International license.

Supplemental material

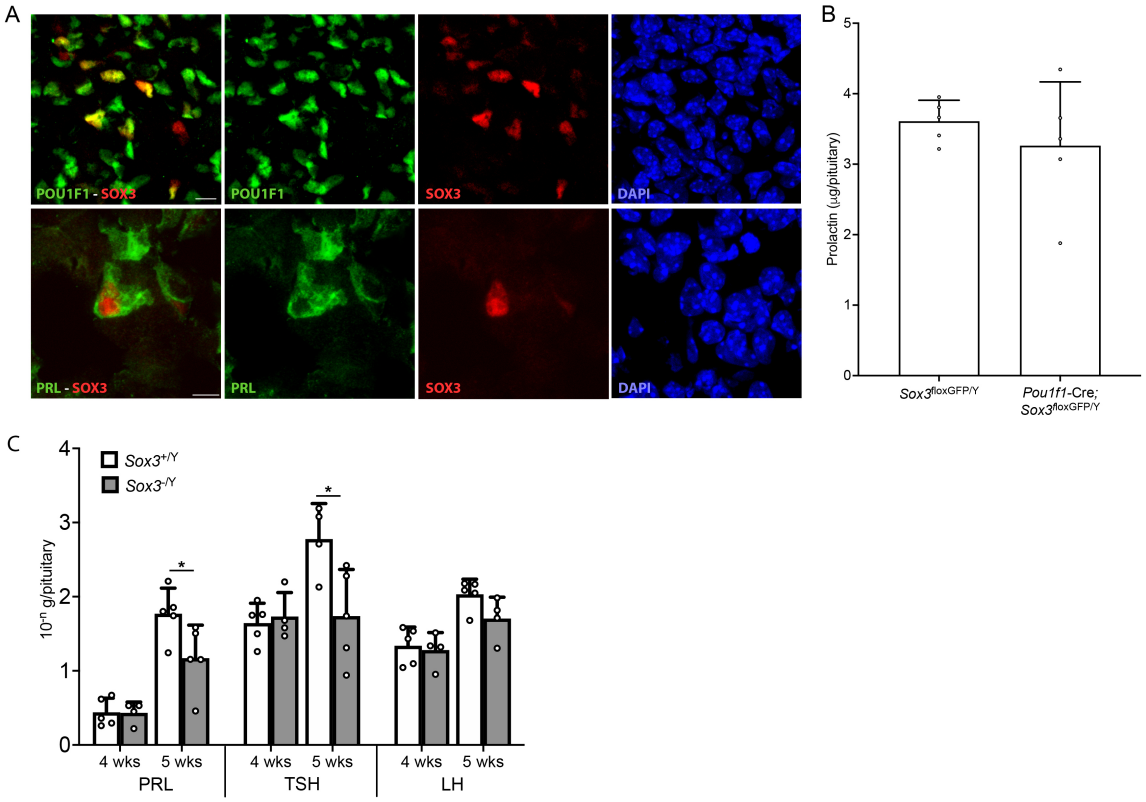

Supplementary Figure 1: Pituitary expression of SOX3 and RIA

(A) Fluorescent immunolabelling for SOX3, POU1F1 and Prolactin (PRL) on 2-month old control anterior pituitaries. Scale bars represent 10µm. (B) PRL contents in 2-month *Sox3*$^{floxGFP/Y}$ and *Pou1f1*-Cre*; Sox3*$^{floxGFP/Y}$. (C) PRL, TSH and LH contents in 4 weeks and 5 weeks *Sox3*$^{+/Y}$ and *Sox3*$^{-/Y}$ pituitaries. Concentrations on the Y axis: LH, 10^{-6}g per pituitary; PRL, 10^{-6}g per pituitary; TSH, 10^{-7}g per pituitary.
*: $p<0.05$

bioRxiv preprint doi: https://doi.org/10.1101/2023.07.26.550616; this version posted July 28, 2023. The copyright holder for this preprint (which was not certified by peer review) is the author/funder, who has granted bioRxiv a license to display the preprint in perpetuity. It is made available under aCC-BY 4.0 International license.

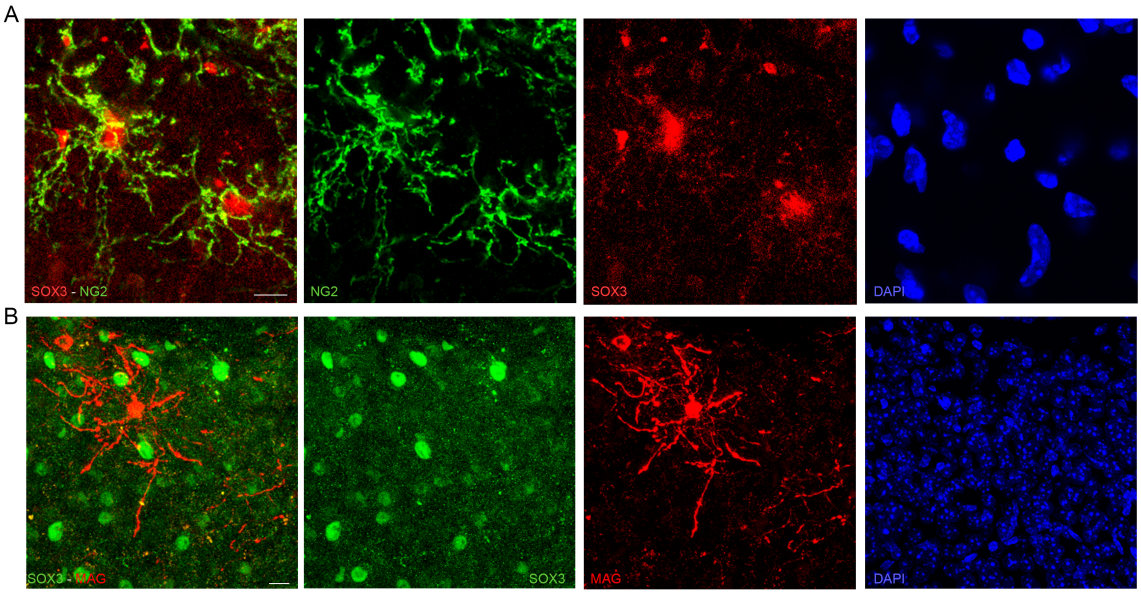

Supplementary Figure 2: Median eminence expression of SOX3

(A-B) Fluorescent immunolabelling for SOX3, NG2 (A) and MAG (B) on 2-month control MEs. SOX3 is expressed in $NG2^{+ve}$ NG2-glia but not in MAG^{+ve} mature oligodendrocytes. Scale bars represent 10µm.

bioRxiv preprint doi: https://doi.org/10.1101/2023.07.26.550616; this version posted July 28, 2023. The copyright holder for this preprint (which was not certified by peer review) is the author/funder, who has granted bioRxiv a license to display the preprint in perpetuity. It is made available under aCC-BY 4.0 International license.

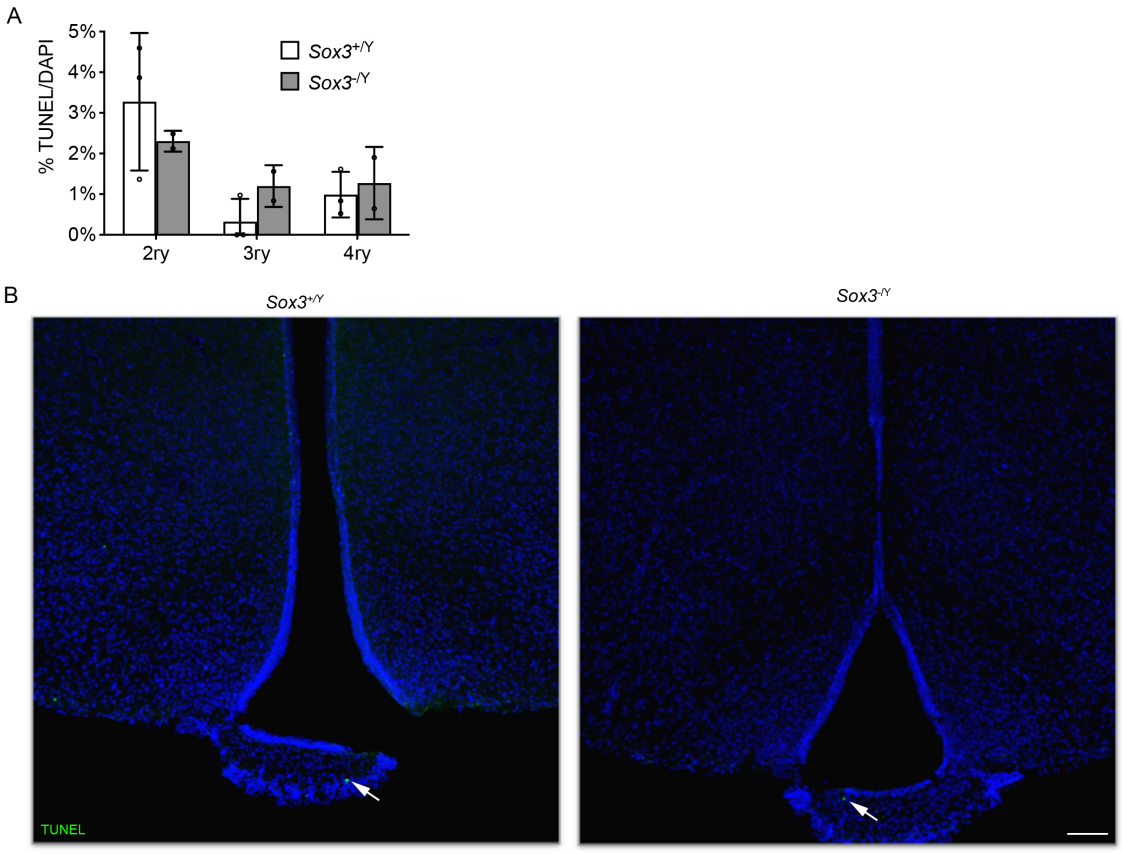

Supplementary Figure 3: Post-weaning apoptosis analysis *in vitro* and *in vivo*

(A) Percentage of TUNEL^{+ve} cells in control (white columns) and *Sox3*$^{-/Y}$ (grey columns) of monolayer cultures derived from adult animals at secondary, tertiary, and quaternary passages. No significant difference is observed. (B) TUNEL staining on control and *Sox3*$^{-/Y}$ 2-month hypothalami. Arrows point to TUNEL^{+ve} cells. Very few positive cells are present in both samples. Scale bar represents 100µm.

bioRxiv preprint doi: https://doi.org/10.1101/2023.07.26.550616; this version posted July 28, 2023. The copyright holder for this preprint (which was not certified by peer review) is the author/funder, who has granted bioRxiv a license to display the preprint in perpetuity. It is made available under aCC-BY 4.0 International license.

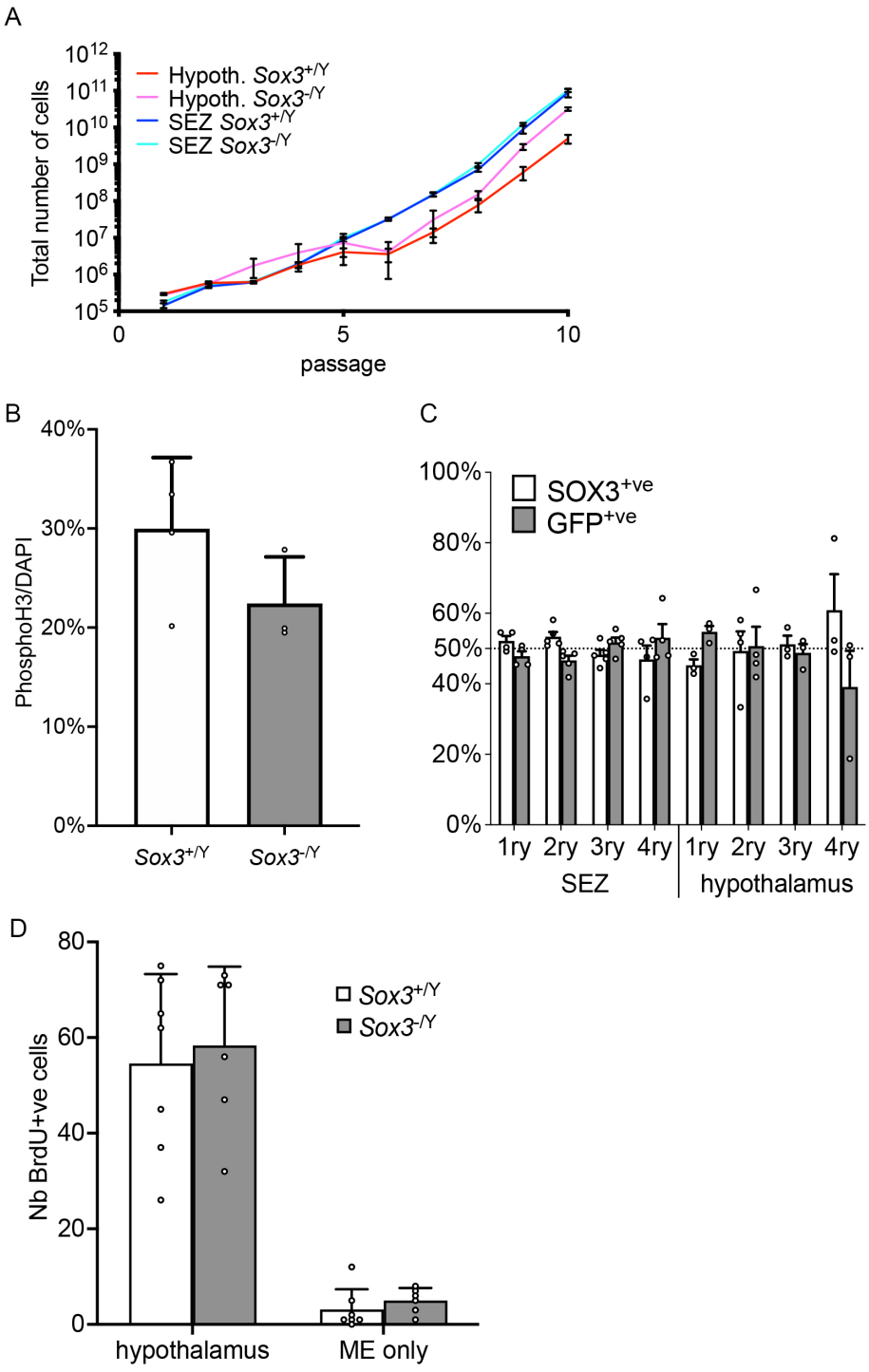

Supplementary Figure 4: Pre-weaning hypothalamic neural/progenitor cells analyses *in vitro* and *in vivo*

bioRxiv preprint doi: https://doi.org/10.1101/2023.07.26.550616; this version posted July 28, 2023. The copyright holder for this preprint (which was not certified by peer review) is the author/funder, who has granted bioRxiv a license to display the preprint in perpetuity. It is made available under aCC-BY 4.0 International license.

(A) Total number of cells counted after each passage from hypothalamic derived (red/pink) or SEZ derived (dark and light blue) NSCs from ten-day old control (dark blue/red) and *Sox3*-null mice (light blue/pink). *Sox3*-null NSCs from pups self-renew normally. (B) Percentage of phospho-histone $H3^{+ve}$ cells in secondary progenitor monolayer cultures originated from ten-day old control and *Sox3*-null hypothalami. *Sox3*-null progenitors proliferate normally. (C) Percentage of neurospheres containing mostly $SOX3^{+ve}$ cells (white columns) or mostly GFP^{+ve} cells (grey columns) derived from ten-day old $Sox3^{+/\Delta GFP}$ SEZ or hypothalami. *Sox3*-null, GFP^{+ve} progenitors are maintained in these cultures from young females. (D) Number of $BrdU^{+ve}$ cells in one-week control (white columns) and *Sox3*-null (grey columns) hypothalamic parenchymas and MEs. The number of $BrdU^{+ve}$ cells is similar in *Sox3*-null compared to control samples.

bioRxiv preprint doi: https://doi.org/10.1101/2023.07.26.550616; this version posted July 28, 2023. The copyright holder for this preprint (which was not certified by peer review) is the author/funder, who has granted bioRxiv a license to display the preprint in perpetuity. It is made available under aCC-BY 4.0 International license.

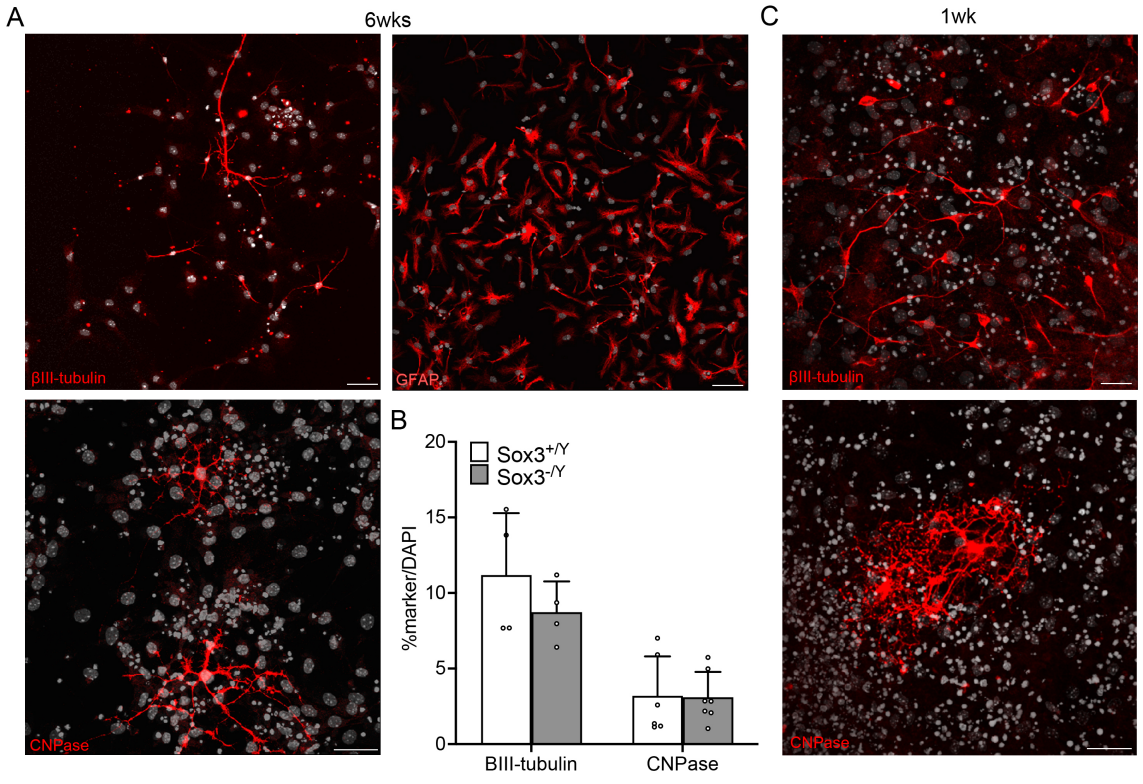

Supplementary Figure 5: hypothalamic neurosphere differentiation potential

(A-C) Fluorescent immunolabelling for GFAP (astrocytes), βIII-tubulin (neurons), CNPase (oligodendrocytes) on 6-weeks (A) and 1-week (C) control hypothalamic differentiated progenitor monolayers. (B) Percentage of cells differentiated into βIII-tubulin^{+ve} neurons and CNPase^{+ve} oligodendrocytes derived from 6-weeks control (white columns) or *Sox3*-null (grey columns) hypothalami. Scale bars represent 30µm.

bioRxiv preprint doi: https://doi.org/10.1101/2023.07.26.550616; this version posted July 28, 2023. The copyright holder for this preprint (which was not certified by peer review) is the author/funder, who has granted bioRxiv a license to display the preprint in perpetuity. It is made available under aCC-BY 4.0 International license.

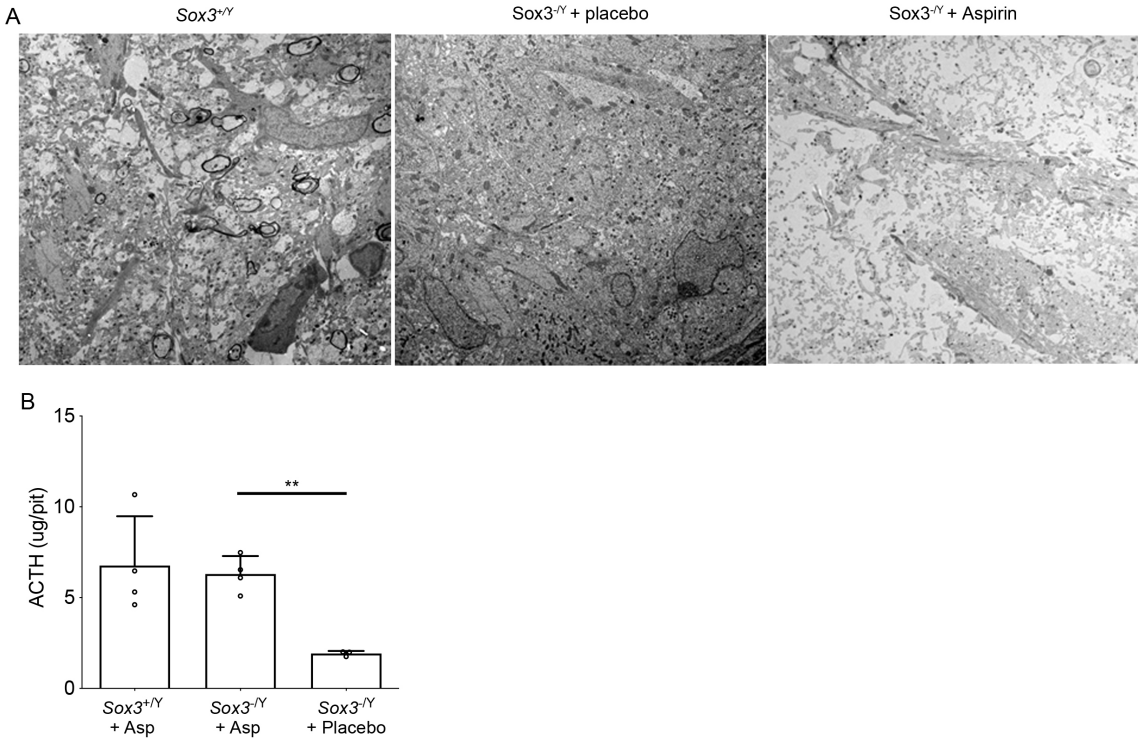

Supplementary Figure 6: low dose aspirin treated *Sox3*-null myelin analyses and RIA

(A) Transmission electron microscopy images of 2-month old control, *Sox3*$^{-/Y}$ with placebo and aspirin-treated *Sox3*$^{-/Y}$ MEs. Myelinated axons are missing in aspirin-treated *Sox3*-null MEs. (B) ACTH contents in 2-month *Sox3*$^{+/Y}$, *Sox3*$^{+/Y}$with low dose aspirin, *Sox3*$^{-/Y}$ with low dose aspirin and *Sox3*$^{-/Y}$ with placebo pituitaries. Note the rescue in ACTH contents in *Sox3*-null mice receiving low dose aspirin.
**: $p<0.01$

bioRxiv preprint doi: https://doi.org/10.1101/2023.07.26.550616; this version posted July 28, 2023. The copyright holder for this preprint (which was not certified by peer review) is the author/funder, who has granted bioRxiv a license to display the preprint in perpetuity. It is made available under aCC-BY 4.0 International license.

Crick (2018S from Envigo)	NIMR (5021 from Labdiet)
Ingredients (in descending order of inclusion)	
Ground wheat	Ground corn
Ground corn	Wheat middling
Wheat middling	Dehulled soybean meal
Dehulled soybean meal	Wheat germ
Corn gluten meal	Fish meal
Soybean oil	Ground wheat
Brewers dried yeast	Porcine animal fat
Salt	Brewers dried yeast
Vitamins	Soybean oil
	Salt
	Vitamins
Macronutrients	
18.6% crude Protein	20% crude protein
6.2% Fat	9% Fat
3.5% crude fiber	5% crude fiber

Supplementary Figure 7: diet composition

Composition of rodent chow at NIMR and Crick.